NUREG/CR-2345, Vol. 2
HEDL-TME 81-34

LWR PRESSURE VESSEL IRRADIATION SURVEILLANCE DOSIMETRY

QUARTERLY PROGRESS REPORT
APRIL 1981 - JUNE 1981

Hanford Engineering Development Laboratory

Preparation coordinated by
G.L. Guthrie
W.N. McElroy

Prepared for the U.S. Nuclear Regulatory Commission

GPO Printed copy price: $5.00

NUREG/CR--2345-Vol.2

DE83 006087

NUREG/CR-2345, Vol. 2
HEDL-TME 81-34
R5

LWR PRESSURE-VESSEL IRRADIATION SURVEILLANCE DOSIMETRY

QUARTERLY PROGRESS REPORT
APRIL 1981 - JUNE 1981

Hanford Engineering Development Laboratory

Operated by Westinghouse Hanford Company
P.O. Box 1970 Richland, WA 99352
A Subsidiary of Westinghouse Electric Corporation

Preparation coordinated by
G.L. Guthrie
W.N. McElroy

Manuscript completed: June 1982
Date published: December 1982

Prepared for Division of Engineering Technology
Office of Nuclear Regulatory Research
U.S. Nuclear Regulatory Commission
Washington, DC 20555
NRC FIN No. B5988-7

FOREWORD

The Light Water Reactor Pressure Vessel Surveillance Dosimetry Improvement Program (LWR-PV-SDIP) was established by NRC to improve, maintain, and standardize neutron dosimetry, damage correlation, and the associated reactor analysis data and procedures that are used to predict the integrated effect of neutron exposure to LWR-PV. A vigorous research effort attacking the same measurment and analysis problems exists worldwide, with strong cooperative links among NRC-supported activities at HEDL, ORNL, NBS, MEA/ENSA and those supported by CEN/SCK (Mol, Belgium), EPRI (Palo Alto, USA), KFA (Jülich, Germany), and several UK laboratories. These cooperative links are strengthened by the active membership of the scientific staff from many participating countries and laboratories in the ASTM E10 Committee on Nuclear Technology and Applications. Several subcommittees of ASTM E10 are responsible for the preparation of LWR-PV surveillance standards.

The primary objective of the multilaboratory program is to prepare an updated and improved set of physics-dosimetry-metallurgy, damage correlation, and associated reactor analysis ASTM Standards for LWR-PV irradiation surveillance programs. Supporting this objective are a series of analytical and experimental validation and calibration studies in "Standard, Reference, and Controlled Environment Benchmark Fields," reactor "Test Regions," and operating power reactor "Surveillance Positions."

These studies will establish and certify the precision and accuracy of the measurement and predictive methods recommended for use in the ASTM Standards. Consistent and accurate measurement and data analysis techniques and methods, therefore, will be developed and validated along with guidelines for required neutron field calculations used to correlate changes in material properties with the characteristics of the neutron radiation field. It is expected that the application of the established ASTM Standards will permit the reporting of measured materials property changes and neutron exposures to an accuracy and precision within bounds of 10 to 30%, depending on the measured metallurgical variable and neutron environment.

The assessment of the radiation-induced degradation of material properties in a power reactor pressure vessel requires accurate definition of the neutron field from the outer region of the reactor core to the outer boundaries of the pressure vessel. Problems with measuring neutron flux and spectrum are associated with two distinct components of LWR-PV irradiation surveillance procedures: 1) proper application of calculational estimates of the neutron fluence delivered to in-vessel surveillance positions, various locations in the vessel wall, and ex-vessel support structures and surveillance positions, and 2) understanding the relationship between material property changes in reactor vessels, in-vessel support structures, and in metallurgical test specimens in test reactors and at accelerated neutron flux positions in operating power reactors.

The first component requires validation and calibration experiments in a variety of neutron irradiation test facilities including LWR-PV mockups, power reactor surveillance positions, and related benchmark neutron fields. The benchmarks serve as a permanent reference measurement for neutron flux and fluence detection techniques, which are continually under development and widely applied by laboratories with different levels of capability. The second component requires a serious extrapolation of an observed neutron-induced mechanical property change from test reactor "Test Regions" and operating power reactor "Surveillance Positions" to locations inside the body of the pressure vessel wall and to ex-vessel support structures. The neutron flux at the vessel inner wall is up to one order of magnitude lower than at surveillance specimen positions and up to two orders of magnitude lower than for test reactor positions. At the vessel outer wall, the neutron flux is one order of magnitude or more lower than at the vessel inner wall. Further, the neutron spectrum at, within, and leaving the vessel is substantially different.

In order to meet the reactor pressure vessel radiation monitoring requirements, a variety of neutron flux and fluence detectors are employed, most of which are passive. Each detector must be validated for application to the higher flux and harder neutron spectrum of the test reactor "Test Region"

and to the lower flux and degraded neutron spectrum at "Surveillance Positions." Required detectors must respond to neutrons of various energies so that multigroup spectra can be determined with accuracy sufficient for adequate damage response estimates. Proposed detectors for the program include radiometric detectors, helium accumulation fluence monitors, solid state track recorders, and damage monitors.

The necessity for pressure vessel mockup facilities for dosimetry investigations and for irradiation of metallurgical specimens was recognized early in the formation of the NRC program. Experimental studies associated with high and low flux versions of a PWR pressure vessel mockup are in progress. The low flux version is known as the Poolside Critical Assembly (PCA) and the high flux version is known as the Poolside Facility (PSF). Both are located at ORNL. As specialized benchmarks, these facilities will provide well-characterized neutron environments where active and passive neutron dosimetry, various types of LWR-PV neutron field calculations, and temperature-controlled metallurgical specimen exposures are brought together.

The results of the measurement and calculational strategies outlined here will be made available for use by the nuclear industry as ASTM Standards. Federal Regulation 10CFR50 already requires adherence to several ASTM Standards that establish a surveillance program for each power reactor and incorporate flux monitors and neutron field evaluation. Revised and new standards in preparation will be carefully up-dated, flexible, and, above all, consistent.

CONTENTS

CONTENTS (Cont'd)

FIGURES

TABLES

ACKNOWLEDGMENTS

The following organizations are presently participating in the Light Water Reactor Pressure Vessel Surveillance Dosimetry Improvement Program and will periodically contribute written reports, experimental data, or calculations.

Atomic Energy Research Establishment (AERE-H), Harwell, UK

Babcock & Wilcox Company (B&W), USA

Battelle Memorial Institute (BMI), Columbus Laboratory, USA

Brookhaven National Laboratory (BNL), USA

Centre d'Étude de l'Energie Nucléaire - Studiecentrum Voor Kernenergie (CEN/SCK), Mol, Belgium

Centre d'Études Nucléaires de Saclay (CEA, Saclay), Gif-sur-Yvette, France

Combustion Engineering, Inc. (CE), USA

EG&G ORTEC, USA

Electric Power Research Institute (EPRI), USA

Engineering Services Associates (ENSA), USA

Fracture Control Corporation (FCC), USA

General Electric Vallecitos Nuclear Center (GE-VNC), USA

Hanford Engineering Development Laboratory (HEDL), USA

Institüt für Kernenergetik und Energiesysteme der Universitat Stuttgart (IKE), Stuttgart, Germany

IRT Corporation (IRT), USA

Italian Atomic Power Authority (ENEL), Italy

Japan Atomic Energy Research Institute (JAERI), Japan

Kernforschungsanlage Jülich Gmbh (KFA), Germany

Kraftwerk Union, Germany

Materials Engineering Associates (MEA), USA

National Bureau of Standards (NBS), USA

Oak Ridge National Laboratory (ORNL), USA

Radiation Research Associates (RRA), USA

Rockwell International Energy Systems Group (RIES), USA

Rolls-Royce and Associates Limited (RRAL), Derby, UK

Science Applications Incorporated (SAI), USA

Ship Research Institute (SRI), Japan

Southwest Research Institute (SWRI), USA

University of Arkansas (UA), USA

University of California, Santa Barbara (UCSB), USA

University of Tennessee (UT), USA

University of Tokyo, Japan

Westinghouse Electric Corporation - Nuclear Technology Division

Westinghouse Electric Corporation - Research and Development Division (WR&D)

SUMMARY

HANFORD ENGINEERING DEVELOPMENT LABORATORY (HEDL)

The FERRET code was used in three types of calculations (A, B, C) to determine the benefit derived from including benchmark field activation data as part of the input information in the neutron unfolding procedure, and the results compared. For Type A calculations, the adjustment code input information included benchmark field activation data for foils of the same type as those irradiated in the PCA unknown test field. Group flux values of the benchmark field, foil cross sections, and a priori input test spectrum were all considered adjustable and were accompanied by appropriate covariance information. For Type B calculations, no benchmark field information was introduced in the unfolding code input, but the a priori group flux values of the test field and radiometric foil group cross sections were both considered adjustable and were accompanied by suitable covariance input information. For Type C calculations, the radiometric foil cross sections were not allowed to vary and only the a priori input test field spectrum was adjustable. Although results from the three types of calculations were essentially the same, use of benchmark field referencing is considered advantageous when benchmark irradiations are used to calibrate the radiometric counting procedure yield smaller activating input uncertainties and guard against gross erros. The guarding against gross errors is by far the most important consideration when considering correlations and applications of derived-measured physics-dosimetry-metallurgy results for LWR power plant surveillance programs.

The Buffalo Light Water Reactor is used by NRL to irradiate metallurgical specimens for measurement of property changes related to LWR-PV. To provide supporting spectral flux-fluence information in those reactor positions utilized by NRL, HEDL prepared two spectral gradient pins for irradiation in a corner and center hole of either the c-2 or b-4 positions used by NRL. After irradiation at ambient temperature for a minimum of 2 days at full power, the pins will be shipped to HEDL for analysis.

Etching and annealing properties of Brazilian quartz crystals are under investigation to determine their suitability for use as SSTR and damage monitors in nuclear reactor environments where temperature and neutron fluences are high. Observer objectivity in counting fission tracks was established at the 1-2% level, and a method of standardizing chemical etching from one sample of quartz to another was found. A method was also found that corrects for track loss due to thermal annealing in terms of the effect that annealing has on track size in the direction of maximum bulk etch rate parallel to the (100) plane, provided the fractional track loss does not exceed ~40%.

OAK RIDGE NATIONAL LABORATORY (ORNL)

ORNL's review of NUREG/CR-1861 was completed.

Results of the REAL-80 program were reviewed and submitted to IAEA.

The effect of concrete instead of water behind the void box of the PCA 4/12 and 4/12 SSC configurations was calculated.

Experimental data from tests made on the second Simulated Surveillance Capsule (SSC-2) were analyzed and the discrete-time optimal control law was implemented into the computer software.

SSC-2 was inserted at 1148, June 1, 1981.

The "ASTM Standard Guide for Application of Neutron Transport Methods for Reactor Vessel Surveillance" will be submitted for simultaneous balloting by the E10 Main Committee and the E10.05 Subcommittee.

A general paper on the "Theory and Practice of General Adjustment and Model Fitting Procedure" is in publication.

A "New Standard Recommended Practice of Neutron Spectrum Adjustment Methods in Reactor Surveillance" was prepared for balloting by the E10.05 Subcommittee.

NAVAL RESEARCH LABORATORY (NRL)

Charpy-V (C_v) notch ductility data are presented for six pressure vessel materials (two reference plates, two forgings, and two weld deposits) contained in Simulated Surveillance Capsule No. 1 (SSC-1) irradiated at 288°C in the NRC Pool Side Facility (PSF). Charpy-V data developed by NRL for the unirradiated condition of one forging are also presented. Brittle/ductile transition temperature elevations by irradiation, indexed by C_v 41J temperatures, ranged from 0°C to 222°C. Material sensitivities to irradiation are compared with prior observations for the ASTM A302-B reference plate and the HSST A533-B Plate 03 irradiated in-core in test reactor experiments.

HANFORD ENGINEERING DEVELOPMENT LABORATORY
(HEDL)

A. EFFECT OF FOIL CROSS-SECTION ADJUSTMENT CONTRAINTS IN FERRET CALCULATIONS OF NEUTRON FIELD INTEGRALS

G. L. Guthrie and D. L. Oberg - HEDL

Objective

The present work has two objectives. The first objective is to determine whether neutron spectrum adjustment calculations can be satisfactorily performed in a simple manner with no adjustment allowed in the radiometric foil cross sections. The second objective is to determine what benefits, acrue from adding benchmark field foil activation information to the adjustment code input.

Results of the present study are useful in writing the ASTM standard on unfolding adjustment calculations and the ASTM standard on extrapolating surveillance information. These standards are required as part of the LWR-PV Surveillance Dosimetry Improvement Program.

Summary

The FERRET code[1] has been used to perform spectrum adjustment calculations for neutron spectra at several positions in the simulated pressure vessel wall in the PCA experiment at ORNL. The adjustment was accomplished for three separate types of input assumptions (A, B, C), giving three separate sets of computer runs (A, B, C). The results were compared. For the Type A computer runs, the adjustment code input information included benchmark field activation data for foils of the same type as those irradiated in the PCA unknown test field. Group flux values of the benchmark field, foil cross sections, and the a priori input test spectrum were all considered adjustable and were accompanied by appropriate covariance information. For Type B computer runs, no benchmark field information was explicitly introduced in the unfolding code input, but the a priori group flux values of the test field and the radiometric foil group cross sections were both considered adjustable and were accompanied by covariance input information. For the

third type of computer runs (Type C), the radiometric foil cross sections were not allowed to vary, and only the a priori input test field spectrum was adjustable. Although results from the three types of calculations were essentially indistinguishable, use of benchmark fields is considered advantageous if the benchmark information is used to calibrate the radiometric counting procedure.

Accomplishments and Status

The FERRET code[1] was used in three separate types of neutron spectrum adjustment calculations to determine the benefit from treating the radiometric foil cross sections as adjustable quantities. Three separate sets of input assumptions were used in the adjustment procedures. The three different types of calculations differed only in the use of the three separate sets of input assumptions, as described in the Summary. One set of input assumptions made use of benchmark field activation data in the input information.

The ability to utilize the benchmark information and to adjust the benchmark field and/or the foil cross sections is a relatively new capability that has become available in the last four years. Previously, the foil cross sections were held fixed and only the unknown test field spectrum was adjusted.

The present study used techniques similar to those used in the PCA Blind Test analysis,[2] with 53 energy groups for the descriptions of the spectra and cross sections. The features of the FERRET code[1] are described elsewhere, but, to create a basic familiarity, we point out that the FERRET code minimizes a "generalized sum of squared residuals"[2] working with a normal distribution in the activations and log normal distributions for the cross sections and a priori group fluxes.

Calculations using the three types of input assumptions (A, B, C) were performed for the PCA 8/7* configuration at the 1/4T, 1/2T, and 3/4T depths in the simulated pressure vessel wall. Input foil activation information was derived from exposures involving the following reactions: $^{237}Np(n,f)$,

$^{103}Rh(n,n')$, $^{115}In(n,n')$, $^{58}Ni(n,p)$, $^{27}Al(n,\alpha)$, $^{238}U(n,f)$ and bare and cadmium-covered $^{235}U(n,f)$. The ^{235}U reactions were monitored by SSTR techniques, while all other measurements indicated above were radiometric. The benchmark field integral statements (Type A calculations) in the code were entered for all the reactions given above except for the SSTR (^{235}U).

The benchmark irradiation activities and their associated uncertainties came from data collected[3] from irradiations in thermally driven ^{235}U fission spectra (reported under "Measured" in Table II of Reference 3).

In any given calculation, the adjustable quantities were associated with covariance matrices. the covariance matrices and the a priori valves of the adjustable input quantities were the same as those used[2] in the PCA Blind Test Report. No use has been made of ^{6}Li or proton recoil spectrometry data in any of the present analyses (A, B, C). The description of these matrices of these matrices is available in Reference 2. The covariance matrices did not contain any negative off-diagonal elements.

For the FERRET[1] input statements regarding the benchmark irradiations, an ENDF/B-V ^{235}U fission spectrum was assumed, and the uncertainties in the group fluxes were those reported by Grundl and Eisenhauer[4] for the segment-adjusted fluxes.

Results of the present study are shown in Table HEDL-1. The quantities $\bar{E}$, ϕ_{TOTAL}, $\phi(E > 0.1$ MeV), $\phi(E > 1.0$ MeV), and dpa/s were calculated for the 1/4T, 1/2T, and 3/4T positions using input assumptions A, B, and C. The similarity of the results for the three sets of input assumptions can be seen by examining the values found for $\phi(E > 1.0$ MeV) at the 1/2T depth, taken as an arbitrary example. When the benchmark field data was explicitly

---

*8/7 refers to the experimental geometry. The distance between the core and the thermal shield is 8 cm, while the distance from the shield to the simulated pressure vessel wall is 7 cm.

TABLE HEDL-1

COMPARISON OF THREE METHODS FOR OBTAINING FOIL CROSS-SECTION ADJUSTMENT CONSTRAINTS IN CALCULATIONS OF COMMON INTEGRAL FLUX QUANTITIES IN THE PCA

Quantity Calculated	Position	Adjusted Results Method A*		Method B**		Method C***	
$\bar{E}$	1/4T	5.454E-01	2.75%	5.446E-01	4.17%	5.499E-01	2.61%
	1/2T	4.758E-01	3.35%	4.768R-01	4.61%	4.800E-01	2.95%
	3/4T	4.369E-01	3.98%	4.391E-01	5.12%	4.403E-01	3.35%
ϕ_{Total}	1/4T	1.657E-06	6.93%	1.652E-06	7.79%	1.641E-06	7.00%
	1/2T	1.008E-06	7.66%	9.964E-07	8.25%	9.940E-07	7.54%
	3/4T	5.500E-07	8.11%	5.406E-07	8.60%	5.523E-07	7.80%
ϕ (E>0.1 MeV)	1/4T	9.227E-07	7.71%	9.178E-07	9.52%	9.086E-07	7.91%
	1/2T	6.122E-07	8.34%	6.018E-07	9.53%	5.998E-07	8.14%
	3/4T	3.503E-07	8.94%	3.423E-07	9.87%	3.436E-07	8.42%
ϕ (E>1.0 MeV)	1/4T	2.809E-07	3.30%	2.809E-07	4.56%	2.830E-07	3.30%
	1/2T	1.354E-07	3.80%	1.348E-07	4.87%	1.360E-07	3.78%
	3/4T	6.153E-08	4.30%	6.123E-08	5.23%	6.167E-08	4.21%
dpa/s ($\times 10^{24}$)	1/4T	4.594E-04	4.00%	4.574E-04	5.40%	4.573E-04	3.94%
	1/2T	2.609E-04	4.84%	2.578E-04	5.96%	2.583E-04	4.52%
	3/4T	1.364E-04	5.58%	1.343E-04	6.54%	1.350E-04	5.03%

*Benchmark field integral measurments are used. Benchmark field radiometric foil activation cross sections and a priori test fields are all adjustable and accompanied by covariance matrices.

**No benchmark integral measurements were used. Foil cross sections are adjustable and accompanied by covariance matrices.

***Foil cross sections fixed.

included, and the benchmark field, foil cross sections, and test field were all considered adjustable (Case A), $\phi(E > 1.0\ MeV) = 1.354 \times 10^{-7}\ n/cm^2/s$. With the benchmark data omitted, but with the foil cross sections considered adjustable (and accompanied by input covariance matrixes) (Case B), $\phi(E > 1.0\ MeV) = 1.348 \times 10^{-7}\ n/cm^2/s$. When the cross sections were fixed and only the test field is adjustable (Case C), $\phi\ (E > 1.0\ MeV) = 1.360 \times 10^{-7}\ n/cm^2/s$ at the PCA 1/2T position.

The ultimate purpose of the neutron spectrum adjustment calculations is to provide information that can be used to estimate reactor pressure vessel toughness. This latter quantity is related to the shift in the nil ductility transition temperature, as determined from Charpy tests. The shift in nil ductility temperature for typical PV steels is approximately proportional to $(\phi t)^{0.3}$. Consequently, if calculations based on the three sets of input assumptions of the present report were used to make separate predictions of nil ductility temperature shift, the preditions would disagree by only $\sim$4 parts per thousand.

Since experimental data for nil ductility shift commonly has a scatter[5] of nearly 10% (rather than $\sim$4 parts per thousand separating nil ductility temperature shifts estimated from the calculations based on the three separate sets of input assumptions), fixed activation cross sections could be used in an adjustment calculation, instead of the more complete set of assumptions of Type A. Apparently, the chief advantage of using the Type A input assumptions over Type C is in the case where exact duplicate foils are used and one or more of the foil sets is exposed in a benchmark field, followed by a laboratory analysis similar to that given to the surveillance dosimeter set. In this case, the benefit lies largely in the fact that such a procedure calibrates the counting facility and any additional benefit gained from actually including the benchmark data in the statistical adjustment procedure is small.

Comments and Conclusions

The use of benchmark field irradiations and/or the inclusion of the associated integral information in the adjustment code input can accomplish two things.

1) It provides a type of covariance information for the foil cross sections. This integral information effectively supplies negative covariance elements in the off-diagonal positions of the covariance matrices of the activation cross sections. The use of the integral information restrains the adjustment procedure and makes it less likely that all group cross sections for any given foil will simultaneously be changed in the same algebraic direction. This can be accomplished alternatively by actually using a covariance matrix that has negative off-diagonal elements, or it can be accomplished by using integral input statements obtained by computation rather than by an actual benchmark irradiation. Adjustment code utility routines for generating covariance matrices do not ordinarily supply negative off-diagonal elements.

2) If benchmark irradiations are performed and the foils are counted by the same equipment and by procedures that are similar to the procedures used for identical foils exposed in the unknown test field, then the benchmark irradiations can be used to calibrate the counting equipment. The extent of the calibration benefit depends partially on the degree of similarity between the test field and benchmark field.

In most LWR surveillance applications, group cross sections of the radiometric foils are probably better known than the a priori input neutron field group fluxes. When this is the case, most of the needed statistical adjustment takes place in the values of the test field group fluxes. Under these circumstances, the adjustment feature for the cross sections is to some extent superfluous, and the calibration benefit mentioned in 2 is the principal advantage of using benchmark fields.*

Results in Table HEDL-1 show an improvement in the calculated uncertainty with the use of Technique A over Technique B, but it might be realized that the listed uncertainties are themselves uncertain and depend only upon the imprecisely chosen input covariance matrices. The adjustment code does not make any normalization correction based on the "goodness" of the fit.

The trend in the calculated standard deviations can be explained. The covariance matrices for the cross sections in Technique B have no negative off-diagonal elements and no credit is given to the accuracy available for an integral quantity. Thus, the uncertainty values given under Technique B are likely to be too large. This uncertainty is reduced in Technique A where a reasonable uncertainty for some integral values is supplied in the input information. The standard deviation reported for Technique C is close to that for Technique A and is sometimes even smaller because there is no contribution in Technique C from the uncertainty in the cross section. The standard deviations calculated by Techniques A and C are comparable, and the discrepancies between the calculated values of the two standard deviations is believed to be less than the error in either standard deviation, especially since none of the calculated standard deviations was corrected for "goodness" of fit.

If an analyst chooses to allow an adjustment of the cross sections in a neutron field adjustment calculation, then logical consistency would dictate that the adjusted values should be used as the a priori input values of the next adjustment calculation performed, and the covariance matrix for the cross sections should be a revised covariance matrix that resulted from the previous calculation. After the same cross sections have been adjusted several times, the accuracy indicated by the cross section covariance matrix should be so great as to disallow any further major shifts in the cross sections. At that point the results of additional calculations would be essentially the same whether the cross sections were adjustable or not.

---

*In an adjustment calculation where the cross sections are not well known and have not been subjected to numerous previous evaluations and adjustments, the conclusions of the present analysis do not apply.

To some extent this phenomenon has already operated. The present study indicates that tabulated group cross sections have already been adjusted so that the errors are small or cancel to a large extent when the cross sections are used to calculate common integral in fields of the type found in a PV wall. If the cross sections are allowed to "float", the use of benchmark information in the adjustment code input could become important if the other data in the problem contained unexpected gross errors. In such a case, the errors in the other data would cause the code to incorrectly adjust the cross sections and the benchmark data integral statements would inhibit the incorrect cross-section adjustments. This type of difficulty can also be avoided by keeping the cross sections fixed. A better use of benchmark activation data is in uncovering errors before the data is entered into the adjustment code.

Undoubtedly, benchmarking for counting calibration purposes is valuable.

Expected Future Accomplishments

No more work in this explicit area is currently anticipated.

References

1. F. A. Schmittroth, "A Method for Data Evaluation with Lognormal Distributions, Nucl. Sci. & Eng. 72, pp. 19-34, 1979.

2. E. P. Lippincott, F. A. Schmittroth, D. L. Oberg, W. N. McElroy, and R. Gold, "Consistency of Experimental Data and Derived Exposure Parameters Based on Least Squares Analysis," PCA Experiments and Blind Test, W. N. McElroy, Ed., NUREG/CR-1861, HEDL-TME 80-87, pp. 4.2-1, Nuclear Regulatory Commission, Washington, DC, July 1981.

3. A. Fabry, W. N. McElroy, L. S. Kellogg, E. P. Lippincott, J. A. Grundl, D. M. Gilliam and G. E. Hansen, "Review of Microscopic Integral Cross-Section Data in Fundamental Reactor Dosimetry Benchmark Neutron Fields," Neutron Cross Sections for Reactor Dosimetry, IAEA-208, International Atomic Energy Agency, Vienna, Austria, p. 233, 1978.

4. J. Grundl and C. Eisenhauer, "Benchmark Neutron Fields for Reactor Dosimetry in IAEA-208," Proceeding of IAEA Dosimetry Conference, Vienna, Austria, November 1976.

5. G. L. Guthrie, "The Effect of Minor Elements on the Irradiation Embrittlement of Reactor Pressure Vessel Plate Metal - Fluence Dependence," LWR Pressure Vessel Irradiation Surveillance Dosimetry - Quarterly Progress Report for July-September 1979, NUREG/CR-1240, Volume III, HEDL-TME 80-2, Nuclear Regulatory Commission, Washington, DC, December 1980.

B. BUFFALO REACTOR DOSIMETRY IRRADIATION

L. S. Kellogg, E. P. Lippincott, and J. A. Ulseth - HEDL

Objective

To provide supporting spectral and flux-fluence information for data correlation of metallurgical measurements made by the Naval Research Laboratory (NRL).

Summary

The Buffalo Light Water Reactor is used by NRL to irradiate metallurgical specimens for measurement of property changes related to LWR-PVs. To provide supporting spectral flux-fluence information in reactor positions utilized by NRL, HEDL prepared two spectral gradient pins for irradiation in a corner and center hole of either the c-2 or b-4 positions (Figure 1) used by NRL. After irradiation at ambient temperature for a minimum of 2 days at full power, the pins will be shipped to HEDL for analysis.

Accomplishments and Status

Two dosimetry pins were fabricated to NRL specifications (Figure 2). Each was loaded with a Cd-encapsulated spectral set consisting of 7 dosimetry materials and 6 gradient sets consisting of 4 monitors (Figure 3 and Tables 3-6). Quality Assurance (QA) information for the dosimetry materials is provided in Table 2. Capsule welds were qualified in accordance with RDT F6-2T, Section 8, Category 5. Tangential radiographs at four angles of each weld and one overall radiograph were provided to NRL. To satisfy QA Level 3 fabrication requirements, leak checks were made to determine no leaks existed >1 x 10^{-8} std cm^3/s He.

Expected Accomplishments

Irradiated dosimetry materials will be analyzed, and spectral flux-fluence determinations will be made. This information will then be compared with data used by NRL for their metallurgical correlations.

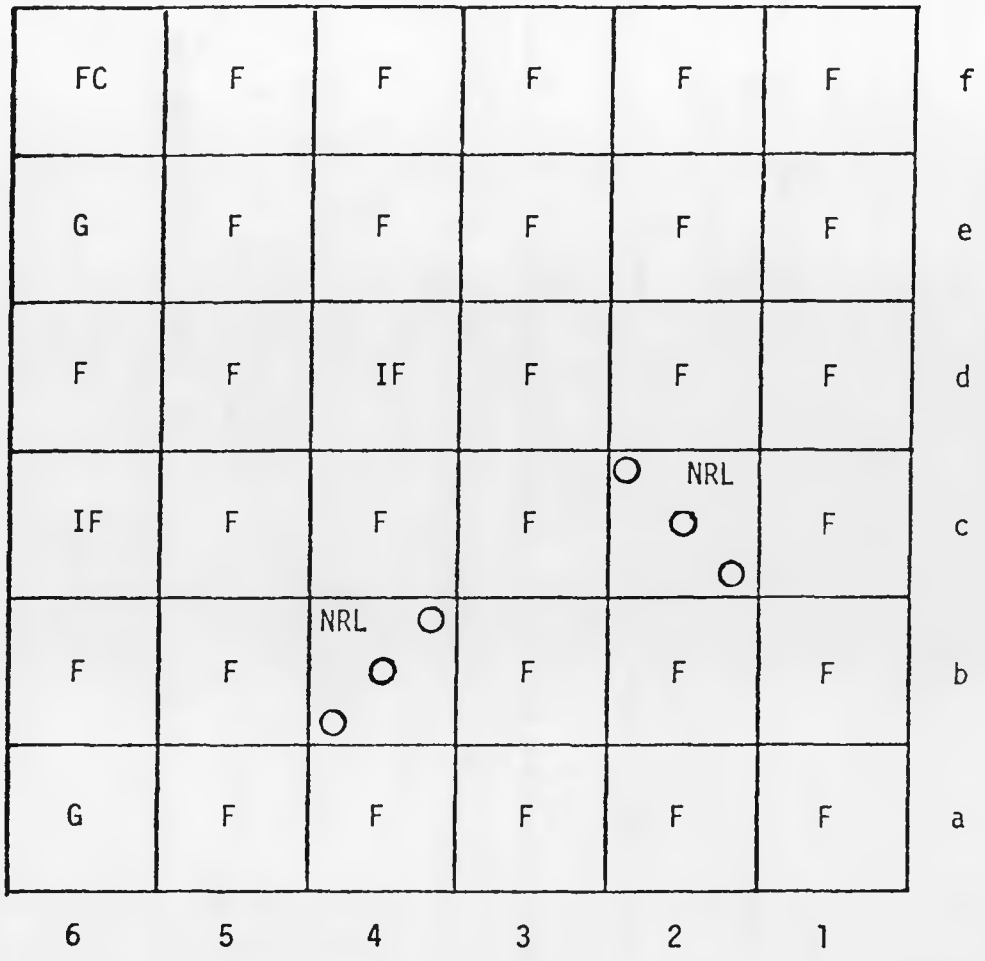

LEGEND

NRL - NRL Irradiation Positions
FC - Fission Chambers
IF - Isotope Facilities
G - Graphite Assemblies
F - Fuel Assemblies

FIGURE HEDL-1. Buffalo LWR Core Configuration.

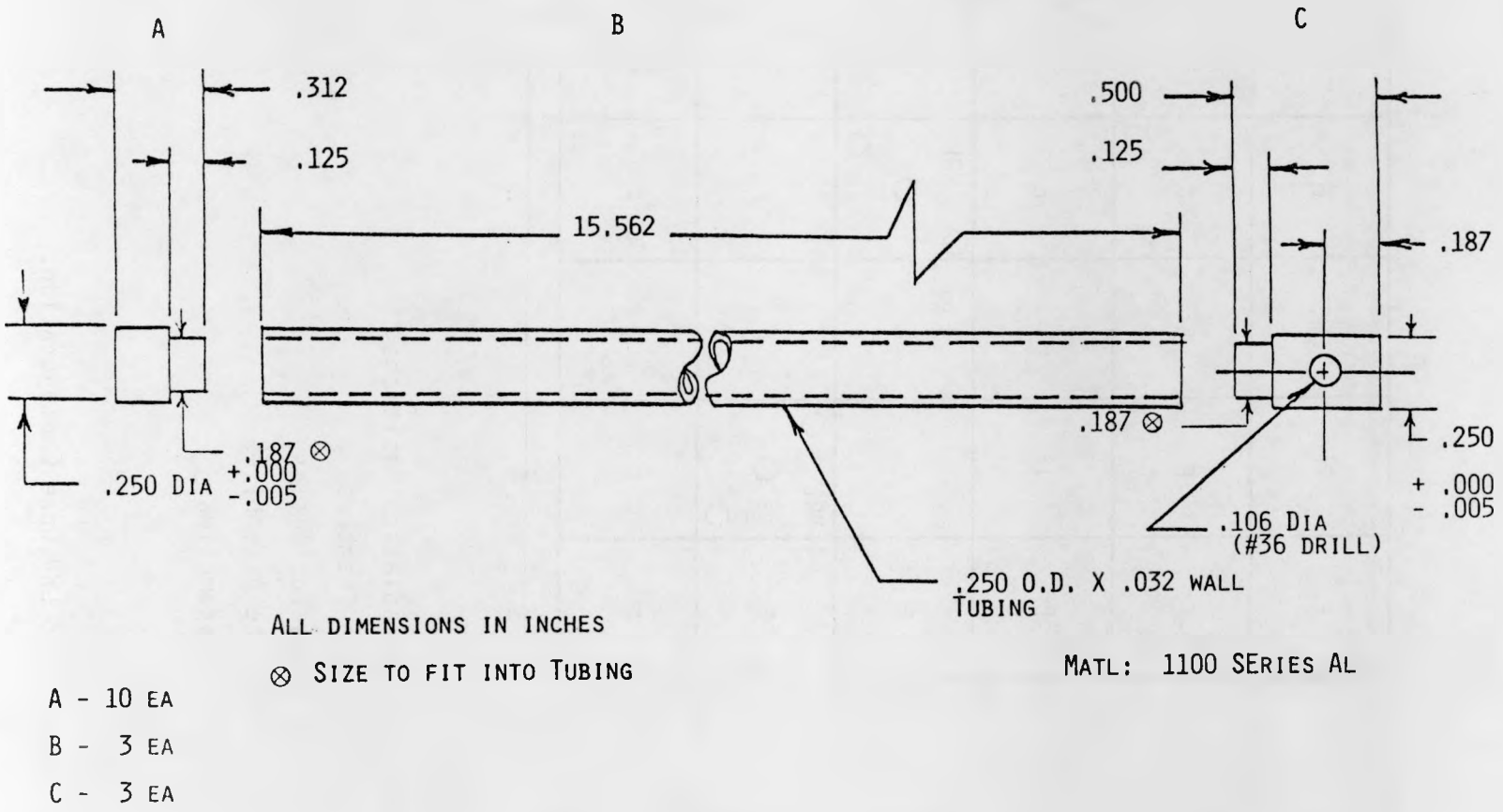

FIGURE HEDL-2. Dosimetry Monitor Tube.

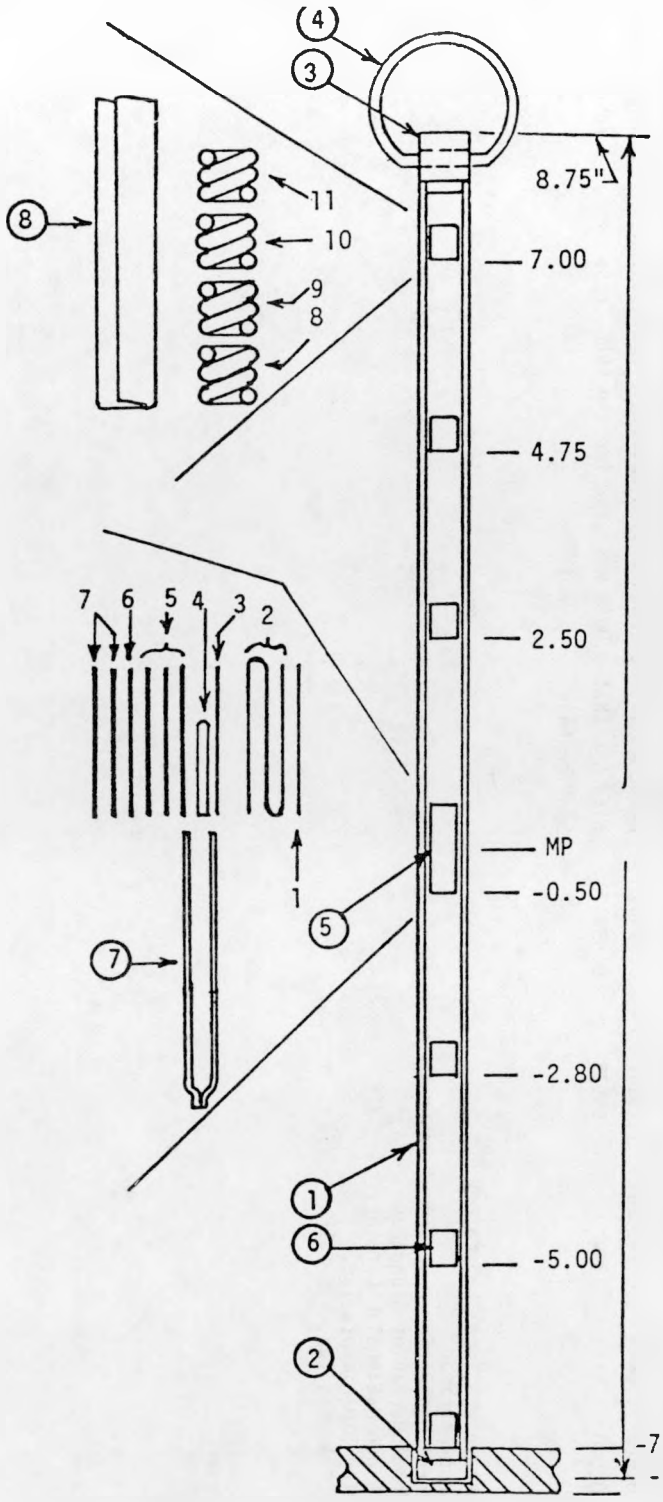

PARTS

(1) Al tube - 0.250" OD x 0.030" wall x 15.56" L

(2) Al bottom end plug - 0.250" D x 0.312" L

(3) Al top end plug - 0.250" D x 0.500 L

(4) Al bail - 1/16" D wire formed into a 1.5"D loop

(5) Spectral Set in 0.020" thick Cd wrap

(6) Gradient Set (4 wire coils in Al foil) Pkg. is 0.3" L x 0.13" D- 6 per pin

(7) Cd capsule - 0.13 D x 1" L

(8) Al wrap for the Gradient Sets - 0.001" thick foil

DOSIMETERS

Spectral set

No.	Material	Description
1	0.116%Co/Al	0.020" D wire x 0.5" L
2	Fe	" " x 1.5" L
3	0.145%Ag/Al	" " x 0.5" L
4	$^{237}NpO_2$ in V	V Cap. is 0.280" L x 0.035" OD
5	Ti (3/ Cap.)	0.020" D wire x 0.5" L
6	Ni	" " x "
7	Cu	" " x "

Gradient Sets

8	Fe	0.020" D x 1" L
9	0.116%Co/Al	" x "
10	Ni	" x "
11	0.145%Ag/Al	" x "

Note: The Gradient Sets are loaded upside down below midplane (MP) for a mirror image placement with the above-MP Gradient Sets.

FIGURE HEDL-3. Dosimeter Loading for the Buffalo Reactor Irradiation Experiment (2 pins).

TABLE HEDL-2

QA DATA ON DOSIMETRY MATERIALS

Material	Wire (in.)	Vendor	Batch No.	Purchase Order No.	Elemental Wt Fraction	Isotopic Atom Fraction					Confirmation
						235	236	237	238	239	
$^{237}NpO_2$	0.013	ORNL	NP-24-HP	34462	0.874	<0.000005	<0.000005	≤0.9999	≤0.00003	≤0.000003	ORNL-HEDL
Ag/Al	0.020	RX	Rx70W	03783	0.00145	Natural isotopic composition for target element of all					HEDL
Co/Al	0.020	NBS	SRM953	89085	0.00116	nonfissile materials are those recommended in "Atomic					NBS
Ni	0.020	SE	NA "I"	"1"	0.99999	Weights of the Elements 1977," Vol. 51, pp. 405-433,					Vendor
Fe	0.020	RX	SC-53	19046	0.99999	Pure & Appl. Chem. (1979) with the exception of ^{58}Fe					Vendor
Cu	0.020	CA	CPI-3054	19047	0.99999	where it was determined in a private communication					Vendor-HEDL
Ti	0.020	RX	139W	69925	0.99917	with BNL that 0.0033 was used for the ENDF Cross					Vendor
						Section File.					

ACRONYMS

BNL = Brookhaven National Laboratory
CA = Cominco American
HEDL = Hanford Engineering Development Laboratory
NBS = National Bureau of Standards
ORNL = Oak Ridge National Laboratory
RX = Reactor Experiments Inc.
SE = Semi Elements Inc.

TABLE HEDL-3

BUFFALO LWR IRRADIATION EXPERIMENT - CAPSULE ONE (MIDPLANE)

Material	Purchase Order Number	Batch Number	Description	Material Wt., mg	Encapsulated Monitor Description					
					In	Wt., mg	Dia.	Length	Ident.	Remarks
Ag/Al	03783	Roll A	0.020"D x 0.500"L Wire	6.620						Al Wrapped 0.145% Ag
Ni	1	Roll 2	" " "	21.80						
Co/Al		Box 1A	" " "	7.469						NBS 0.116% Co
Fe	70804	2	" 1.500" "	64.39						
Cu	19047	CPO 3054	" 0.500" "	44.60						two wires
Ti	69925	139W	" " "	33.86						three wires
^{237}Np	39462	Np-24-HP	NpO_2 Oxide Wire	6.460	V	25.331	0.035	0.280	VI-N	

Loaded Container Weight - 23.4 g

Container loaded by BLC Date 1/5/81

TABLE HEDL-4

BUFFALO LWR IRRADIATION EXPERIMENT - CAPSULE THREE (MIDPLANE)

Material	Purchase Order Number	Batch Number	Description	Material Wt., mg	Encapsulated Monitor Description					
					In	Wt., mg	Dia.	Length	Ident.	Remarks
Ag/Al	03783	Roll A	0.020"D x 0.500"L Wire	6.581						Al Wrapped 0.145% Ag
Ni	1	Roll 2	" " "	22.00						
Co/Al		Box 1A	" " "	6.553						NBS 0.116% Co
Fe	70804	2	" 1.500" "	64.38						
Cu	19047	CPO 3054	" 0.500" "	45.*						two wires
Ti	69925	139W	" " "	33.814						three wires
^{237}Np	39462	Np-24-HP	NpO_2 Oxide Wire	6.589	V	24.761	0.035	0.280		

* To be weighed after irradiation

Loaded Container Weight - 23.4 g

Container loaded by BLC Date 1/5/81

TABLE HEDL-5

BUFFALO GRADIENT SETS

Set	Wt (mg) Co/Al	Ni	Ag/Al	Fe	Assembled Length
1	14.051	50.70	14.276	47.03	.290"
2	14.491	47.62	14.250	45.95	.300"
3	14.178	48.87	14.150	46.30	.300"
4	14.173	52.75	14.024	45.84	.307"
5	14.075	51.32	13.812	46.37	.320"
6	14.165	48.70	14.405	46.19	.320"
7	14.114	48.35	14.477	47.51	.310"
8	14.056	49.31	14.343	47.58	.320"
9	14.037	48.85	14.518	47.34	.310"
10	14.059	50.55	14.693	46.23	.312"
11	14.188	47.50	14.425	46.78	.300"
12	14.076	50.62	14.077	46.24	.305"

Note 1 Each wire is $\sim$ 1.0" long, wrapped three times around a 0.110" Dia. Mandrel

Note 2 Sets 1-6 are loaded in Pin 1, with Set 1 at the bottom and Set 6 at the top. Sets 7-12 are similarly loaded into Pin 3.

TABLE HEDL-6

ELEMENTAL AND TOTAL PIN WEIGHTS FOR THE BUFFALO REACTOR EXPERIMENT

Total Weight- both pins	46.7 g
Elemental weight- both pins	
Ag	0.268 mg
Ni	638.94 mg
Co	0.213 mg
Fe	688.13 mg
Cu	90.0 mg
Ti	67.674 mg
$^{237}NpO_2$	13.049 mg
V	37.043 mg
Al	45.2 g

C. SELECTED ETCHING AND ANNEALING PROPERTIES OF BRAZILIAN QUARTZ CRYSTALS FOR SOLID STATE TRACK RECORDER APPLICATIONS

James H. Roberts, Raymond Gold and Frank H. Ruddy - HEDL

Objective

Define the limitations of Solid State Track Recorders (SSTR) for surveillance dosimetry in light water reactor pressure vessel (LWR-PV) environments. To this end, Standard IIIB entitled: "Application and Analyses of Solid State Track Recorder (SSTR) Monitors for Reactor Vessel Surveillance" was prepared within the ASTM Master Matrix for LWR-PV Standards E706-79. In particular, a better understanding of annealing effects in SSTR is required in order to establish correction factors for track fading in high temperature applications.

Summary

Etching and annealing properties of Brazilian quartz crystals are under investigation to determine their suitability for use as SSTR and damage monitors in nuclear reactor environments where temperature and neutron fluences are high. Observer objectivity in counting fission tracks was established at the 1-2% level, and a method of standardizing chemical etching from one sample of quartz to another was found.

A method was also found that corrects for track loss due to thermal annealing in terms of the effect that annealing has on the track size in the direction of maximum bulk etch rate parallel to the 100 plane, provided the fractional track loss does not exceed ~40%.

Accomplishments and Status

INTRODUCTION

Brazilian quartz crystals are known for their high purity and resistance to thermal annealing of fission tracks.[1] To investigate the SSTR properties of Brazilian quartz, crystals cut as disks and polished in the 100 and 001 planes were investigated.

These crystals were pre-etched for 10.0 minutes in 47% HF at room temperature and then in 65% boiling NaOH for 25 minutes. Selected pre-etched crystals were then exposed to fission fragments from ^{244}Cm or ^{252}Cf. One face of the disk was placed in direct contact with one of these thin sources, and the other face was exposed in a vacuum to normally incident fission fragments.

After exposure, some crystals were etched in 65% boiling NaOH for various times, and the fission tracks incident isotropically were manually counted. Other samples were thermally annealed for various times and temperatures before etching so that changes in track density and size could be investigated.

CHEMICAL ETCHING AND FISSION TRACK COUNTING

The reproducibility and observer objectivity of manual fission track counting for exposures in the 100 and 001 planes after various etching times in boiling 65% NaOH were investigated. After pre-etching in HF and NaOH and exposure to ^{244}Cm as described above were completed, two samples were etched for 10.0 minutes in the 65% boiling NaOH. Fission tracks in each SSTR sample (one cut in the 100 plane and the other in the 001 plane) were counted by five observers using Nikon LKE microscopes. Each of the two samples was etched for an additional 10.0 minutes, and the counting repeated. This procedure was repeated again for total etching times of 25.0 and 30.0 minutes.

In addition to the track counting after each etch, the lengths <L> of the etched holes in the 001 and 100 planes in the direction of maximum bulk etch rates using normally incident fragments were measured with a digitized filar micrometer eyepiece.

Results for the track counting and for the <L> measurements are presented in Table 7. Results for track counting are generally better for the 100 plane than for the 001 plane. Incidentally, observers were not instructed regarding what to count. Since in both planes, surface imperfections exist, the results indicate that even without significant experience with quartz crystals, agreement is at the 1-2% level for the 100 plane. If the data showing best agreement for four observers is chosen, the sigmas for the 100 plane etched 20 and 25 minutes are 0.73 and 0.79%, respectively. Results comparable to that obtained for muscovite[2] are possible.

TABLE HEDL-7

RESULTS OF FISSION TRACK COUNTING AND TRACK SIZE MEASUREMENTS IN NATURAL QUARTZ CRYSTALS CUT IN THE 100 PLANE AND 001 PLANE

100 Plane

Etching Time (min)	<L>* (μm)	(V_g) max** μm/min	Tracks Counted By Each Observer***					
			1	2	3	4	5	Average
10.0	3.94±0.11	0.394±0.011	2151	2361	2398	2391	2283	2316±103(4.5%)
20.0	8.05±0.27	0.403±0.014	2469	2426	2496	2446	2454	2458±26 (1.1%)
25.0	10.12±0.21	0.405±0.008	2435	2390	2406	2419	2496	2429±41 (1.7%)
30.0	11.39±0.33	0.380±0.011	2438	--	2454	2388	2445	2431±30 (1.22%)

001 Plane

Etching Time (min)	<L>* (μm)	(V_g) max** μm/min	Tracks Counted By Each Observer***					
			1	2	3	4	5	Average
10.0	--	--	2067	2111	2174	2258	1788	2080±178(8.6%)
20.0	1.80±0.13	0.090±0.007	2231	2139	2237	2210	2146	2192±47 (2.1%)
25.0	2.30±0.16	0.092±0.006	2258	2177	2165	2213	2244	2211±41 (1.8%)
30.0	2.66±0.18	0.089±0.006	2154	--	2205	2040	--	2133±84 (4.0%)

*Measured for tracks incident perpendicular to the plane along which the crystal was cut.
**(V_g) max is the maximum bulk etch rate.
***Observers are numbered 1 through 5.

The data for <L> as a function of etching time t for the 100 and <L> 001 planes are plotted in Figure 4 and fitted to linear functions. The significance of the linearity of <L> vs t is that a predetermined value of <L>/<Lo> can always be achieved. First, a relatively short etch time t_s is used to determine $<L>_s$ then by re-etching bring <L> up to the predetermined value, thus standardizing the etch from sample to sample. This linearity also demonstrates the reproducibility of the etching technique being used and that "step etching" is a reliable procedure for quartz crystals. Further studies are in progress.

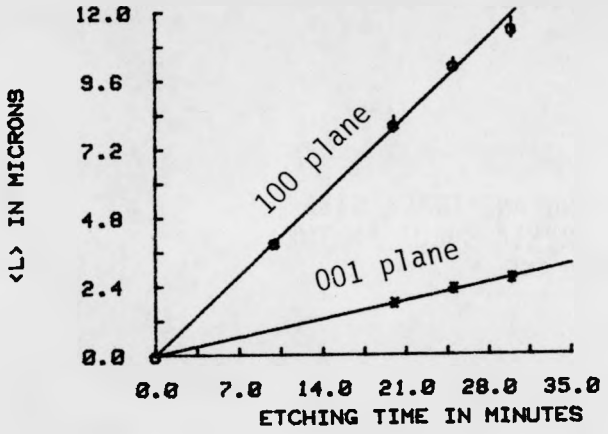

FIGURE HEDL-4. <L> in Direction of Max Bulk Etch Rate in the 100 and 001 Plane. Neg 8106492-2

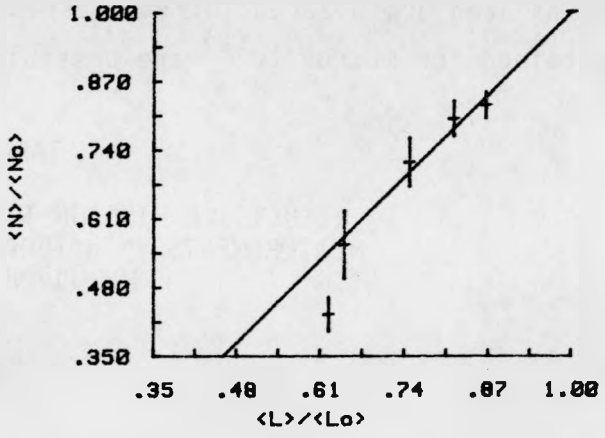

FIGURE HEDL-5. Fraction of Tracks Retained as a Function of <L>/<Lo> in the Thermal Annealing of 100 Quartz.

THERMAL ANNEALING CHARACTERISTICS

In the temperature range projected for using quartz crystals as SSTR in high power reactor environments, it is likely that thermal annealing will be negligible. Combinations of thermal annealing and radiation damage due to high fast neutron fluences, however, will certainly place limits on the usefulness of quartz crystals as SSTR in high power reactor environments.

Only crystals cut in the 100 plane were used in the annealing studies. Samples were exposed to give about 2600 tracks from fission fragments incident isotropically. As before, the other side of the disk was exposed to normally incident full-energy fission fragments. SSTR samples to be heated after exposure were placed between nickel foils in metal capsules. Three samples were heated at a temperature of 857°C for 1.0, 2.0, and 4.0 hours, respectively. The samples were then etched for 20 minutes in 65% boiling NaOH. No tracks were found except in the sample heated for 1.0 hours. Another series was heated for 1, 2, and 4 hours at 837°C. After etching, tracks were found only in the samples heated for 1 and 2 hours. A third run was made at 812°C, with heating times of 1, 2, 4, and 16 hours. Tracks were found in the 1, 2, and 4 hour runs.

Data and results for these annealing experiments are given in Table 8. Tracks were counted by two observers, but the $\langle L \rangle$ were measured by one. The value of $\langle L \rangle$ was measured for 20 normally incident tracks in each sample. A plot of $\langle N \rangle / \langle N_0 \rangle$ vs $\langle L \rangle / \langle L_0 \rangle$ is shown in Figure 5 for the quartz samples in which tracks were revealed. Here $\langle N \rangle$ and $\langle N_0 \rangle$ are the tracks counted in the annealed and unannealed samples, respectively, for the same exposure, and $\langle L \rangle$ and $\langle L_0 \rangle$ are the track lengths in the direction of the maximum bulk etch rates in the 100 plane for the annealed and unannealed samples, respectively. The behavior of $\langle N \rangle / \langle N_0 \rangle$ vs $\langle L \rangle / \langle L_0 \rangle$ is linear in the region $\langle L \rangle / \langle L_0 \rangle \geq 0.65$. In this limited domain, $\langle L \rangle / \langle L_0 \rangle$ is found to be a good parameter to predict track loss.

Further work is in progress to give a more complete annealing characterization of fission tracks in natural quartz, including the combined effects of annealing and radiation damage due to high fluences of fast neutrons. It would appear that these techniques will be of value in correcting for track loss due to annealing in fission track dating research.

TABLE HEDL-8

THERMAL ANNEALING DATA FOR CRYSTALS CUT IN THE 100 PLANE

Sample Number	Heating Time (min)	Temperature (°C)	Obs. 1	Obs. 2	Average	<L> (μm)
A0	0	857	2611	2635	2623	7.84±0.21
A1	60	857	2073	2111	2093	6.40±0.53
A4	0	837	2529	2535	2532	9.87±0.26
A5	63	837	2139	2013	2085	8.55±0.32
A6	123	837	1033	1134	1084	6.15±0.43
AN3	0	812	2606	2504	2555	8.52±0.27
AN1	120	812	1861	1793	1827	6.37±0.58
AN8	240	812	1459	1399	1429	5.51±0.86

Expected Accomplishments

Analytical and experimental efforts are underway to define the annealing limitations of mica and quartz crystal SSTR. Here, the goal is the precise quantification of correction factors for track fading so that the accuracy of low temperature SSTR work can be extended without compromise to high temperature LWR-PV. Combined effects of both annealing and radiation damage produced in the SSTR at high neutron fluence will also be investigated.

REFERENCES

1. R. L. Fleischer, P. B. Price and R. M. Walker, Nuclear Tracks in Solids: Principles and Applications, University of California Press, Berkeley, CA, 1975.

2. R. Gold, R. J. Armani and J. H. Roberts, "Absolute Fission Rate Measurements with Solid State Track Recorders," Nucl. Sci. Eng. 34, pp. 13-32, 1968.

OAK RIDGE NATIONAL LABORATORY
(ORNL)

ORNL-2

A. LIGHT WATER REACTOR PRESSURE VESSEL (LWR-PV) BENCHMARK FACILITIES (PCA, ORR-PSF, ORR-SDMF) AT ORNL

F. B. K. Kam
F. W. Stallmann
L. F. Miller

Objectives

In order to serve as benchmarks, the neutron fields at PCA, ORR-PSF, and ORR-SDMF need to be known and controlled with sufficiently narrow uncertainty bounds. To achieve this objective, extensive measurements are combined with neutron physics calculations. Statistical uncertainty analysis and spectral adjustment techniques are used to determine uncertainty bounds. The results of this task will have a direct impact in the preparation of ASTM Standard for Surveillance of Nuclear Reactor Pressure Vessels. The objectives of these benchmark fields are:

1) PCA (in operation)--to validate and improve neutron transport calculations and dosimetry techniques in LWR-PV environments;
2) ORR-PSF (in operation)--to obtain reliable information from dosimetry measurements and neutron transport calculations and to correlate the spectral parameters with structural changes in the pressure vessel;
3) ORR-SDMF--to investigate results of current surveillance capsules so that dosimetry methods applied by vendors and service laboratories can be:
   a) validated and certified;
   b) improved by development of supplementary experimental data; and
   c) evaluated in terms of actual uncertainties.

A.1 Pressure Vessel Benchmark Facility for Improvement and Validation of LWR Physics Calculations and Dosimetry (PCA)

Accomplishments and Status

Final ORNL review of NUREG/CR-1861, "LWR Pressure Vessel Surveillance Dosimetry Improvement Program: PCA Experiments and Blind Test" has been completed.

All results of the REAL-80 program have been reviewed and submitted to IAEA.

A cross-section library, which includes the elements of concrete, has been generated for the PCA 4/12 and 4/12 + SSC configurations.

One-dimensional (1-D) transport calculations of the PCA 4/12 and 4/12 + SSC have been completed with a concrete slab behind the void box. The results are compared in Tables 1 and 2 against 1-D calculations with water behind the void box.

Table ORNL-1

Comparison of 4/12 Configuration Results

Location	Parameter	Concrete Behind Void Box	Water Behind Void Box	Ratio of Concrete to Water Results
	Np-237 FX	9.084(−26)	9.084(−26)	
	Rh-103 NY	3.670(−26)	3.670(−26)	
	U-238 FX	1.400(−26)	1.400(−26)	
A1	In-115 NX	8.040(−27)	8.040(−27)	1.00
	Ni-58 PX	4.559(−27)	4.559(−27)	
	Fe-54 PX	3.447(−27)	3.447(−27)	
	Al-27 AX	3.092(−29)	3.092(−29)	
	ϕ>1 MeV	3.30(−2)	3.30(−2)	
	Np-237 FX	7.883(−27)	7.883(−27)	
	Rh-103 NY	3.228(−27)	3.228(−27)	
	U-238 FX	1.171(−27)	1.171(−27)	
SSC	In-115 NX	6.765(−28)	6.765(−28)	1.00
	Ni-58 PX	3.797(−28)	3.797(−28)	
	Fe-54 PX	2.880(−28)	2.880(−28)	
	Al-27 AX	3.299(−30)	3.299(−30)	
	ϕ>1 MeV	2.82(−3)	2.82(−3)	
	Np-237 FX	2.747(−27)	2.746(−27)	
	Rh-103 NY	1.022(−27)	1.022(−27)	
	U-238 FX	4.048(−28)	4.048(−28)	
A3	In-115 NX	2.266(−28)	2.266(−28)	1.00
	Ni-58 PX	1.430(−28)	1.430(−28)	
	Fe-54 PX	1.105(−28)	1.105(−28)	
	Al-27 AX	1.481(−30)	1.481(−30)	
	ϕ>1 MeV	9.16(−4)	9.16(−4)	
	Np-237 FX	8.436(−28)	8.404(−28)	
	Rh-103 NY	4.021(−28)	4.007(−28)	
	U-238 FX	1.143(−28)	1.143(−28)	
	In-115 NX	7.058(−29)	7.052(−29)	
A4	Ni-58 PX	3.213(−29)	3.213(−29)	1.00
	Fe-54 PX	2.373(−29)	2.372(−29)	
	Al-27 AX	3.320(−31)	3.320(−31)	
	ϕ>1 MeV	3.17(−4)	3.17(−4)	

Table ORNL-1 (Cont'd)

Location	Parameter	Concrete Behind Void Box	Water Behind Void Box	Ratio of Concrete to Water Results
	NP-237 FX	4.510(−28)	4.450(−28)	1.01
	Rh-103 NY	2.073(−28)	2.047(−28)	1.01
	U-238 FX	4.650(−29)	4.641(−29)	1.00
A5	In-115 NX	3.084(−29)	3.071(−29)	1.00
	Ni-58 PX	1.176(−29)	1.175(−29)	1.00
	Fe-54 PX	8.463(−30)	8.457(−30)	1.00
	Al-27 AX	1.248(−31)	1.248(−31)	1.00
	ϕ>1 MeV	1.44(−4)	1.43(−4)	1.01
	Np-237 FX	2.330(−28)	2.215(−28)	1.05
	Rh-103 NY	1.041(−28)	9.905(−29)	1.05
	U-238 FX	1.795(−29)	1.768(−29)	1.02
A6	In-115 NX	1.294(−29)	1.265(−29)	1.02
	Ni-58 PX	4.120(−30)	4.084(−30)	1.01
	Fe-54 PX	2.883(−30)	2.864(−30)	1.01
	Al-27 AX	4.508(−32)	4.501(−32)	1.00
	ϕ>1 MeV	6.15(−5)	6.02(−5)	1.02
	Np-237 FX	1.137(−28)	8.907(−29)	1.28
	Rh-103 NY	4.930(−29)	3.705(−29)	1.33
	U-238 FX	6.588(−30)	5.477(−30)	1.20
A7	In-115 NX	5.165(−30)	4.181(−30)	1.24
	Ni-58 PX	1.444(−30)	1.260(−30)	1.15
	Fe-54 PX	9.946(−31)	8.832(−31)	1.13
	Al-27 AX	1.625(−32)	1.576(−32)	1.03
	ϕ>1 MeV	2.42(−5)	1.98(−5)	1.22

Table ORNL-2

Comparison of 4/12 + SSC Configuration Results

Location	Parameter	Concrete Behind Void Box	Water Behind Void Box	Ratio of Concrete to Water Results
A1	Np-237 FX	9.129(−26)	9.129(−26)	1.00
	Rh-103 NY	3.685(−26)	3.685(−26)	
	U-238 FX	1.402(−26)	1.402(−26)	
	In-115 NX	8.060(−27)	8.060(−27)	
	Ni-58 PX	4.563(−27)	4.563(−27)	
	Fe-54 PX	3.450(−27)	3.450(−27)	
	Al-27 AX	3.093(−29)	3.093(−29)	
	ϕ>1 MeV	3.31(−2)	3.31(−2)	
SSC	Np-237 FX	1.266(−26)	1.266(−26)	1.00
	Rh-103 NY	5.901(−27)	5.901(−27)	
	U-238 FX	1.605(−27)	1.605(−27)	
	In-115 NX	1.021(−27)	1.021(−27)	
	Ni-58 PX	4.151(−28)	4.151(−28)	
	Fe-54 PX	2.984(−28)	2.984(−28)	
	Al-27 AX	2.955(−30)	2.955(−30)	
	ϕ>1 MeV	4.70(−3)	4.70(−3)	
A3	Np-237 FX	3.158(−27)	3.157(−27)	1.00
	Rh-103 NY	1.283(−27)	1.283(−27)	
	U-238 FX	4.062(−28)	4.062(−28)	
	In-115 NX	2.437(−28)	2.437(−28)	
	Ni-58 PX	1.207(−28)	1.207(−28)	
	Fe-54 PX	8.999(−29)	8.999(−29)	
	Al-27 AX	1.100(−30)	1.100(−30)	
	ϕ>1 MeV	1.06(−3)	1.06(−3)	
	Np-237 FX	1.009(−27)	1.005(−27)	
	Rh-103 NY	4.582(−28)	4.564(−28)	
	U-238 FX	1.060(−28)	1.060(−28)	
	In-115 NX	6.986(−29)	6.980(−29)	
	Ni-58 PX	2.596(−29)	2.596(−29)	
	Fe-54 PX	1.847(−29)	1.847(−29)	
	Al-27 AX	2.404(−31)	2.404(−31)	
	ϕ>1 MeV	3.25(−4)	3.25(−4)	

Table ORNL-2 (Cont'd)

Location	Parameter	Concrete Behind Void Box	Water Behind Void Box	Ratio of Concrete to Water Results
	Np-237 FX	5.440(−28)	5.366(−28)	1.01
	Rh-103 NY	2.411(−28)	2.378(−28)	1.01
	U-238 FX	4.287(−29)	4.279(−29)	1.00
A5	In-115 NX	3.073(−29)	3.060(−29)	1.00
	Ni-58 PX	9.484(−30)	9.475(−30)	1.00
	Fe-54 PX	6.548(−30)	6.544(−30)	1.00
	Al-27 AX	9.007(−32)	9.005(−32)	1.00
	ϕ>1 MeV	1.46(−4)	1.46(−3)	1.00
	Np-237 FX	2.846(−28)	2.705(−28)	1.05
	Rh-103 NY	1.237(−28)	1.175(−28)	1.05
	U-238 FX	1.652(−29)	1.628(−29)	1.01
A6	In-115 NX	1.306(−29)	1.276(−29)	1.02
	Ni-58 PX	3.325(−30)	3.296(−30)	1.01
	Fe-54 PX	2.222(−30)	2.208(−30)	1.01
	Al-27 AX	3.249(−32)	3.244(−32)	1.00
	ϕ>1 MeV	6.25(−5)	6.13(−5)	1.02
	Np-237 FX	1.407(−28)	1.115(−28)	1.26
	Rh-103 NY	5.985(−29)	4.473(−29)	1.33
	U-238 FX	6.047(−30)	5.043(−30)	1.20
A7	In-115 NX	5.270(−30)	4.278(−30)	1.23
	Ni-58 PX	1.1 1(−30)	1.013(−30)	1.15
	Fe-54 PX	7.615(−31)	6.762(−31)	1.13
	Al-27 AX	1.171(−32)	1.136(−32)	1.03
	ϕ>1 MeV	2.46(−5)	2.03(−5)	1.21

A.2 Pressure Vessel Benchmark Facility for LWR Metallurgical Testing of Reactor Pressure Vessel Steels (ORR-PSF)

Accomplishments and Status

Experimental data were obtained and analyzed in order to implement a discrete-time optimal control law for the Second Surveillance Capsule (SSC-2). The experiment on SSC-2 involved changing the electrical heater power of each individual heater, and of combinations of heaters. Variations of individual heater powers were sustained for one hour so that equilibrium conditions could be identified. Variations of combinations of heater powers were sustained for twelve minutes so that dynamical and coupling characteristics could be identified. Steady-state characterization data are shown in Table 3. These data illustrate the change in temperature of each thermcouple due to a one hundred watt change in electrical heater power. Heater power perturbations associated with this experiment are also given by Table 3. The reference temperature of each thermocouple was 34.5°C. Results from the analysis of the dynamical characterization data are not shown since some of the software required for implementation of this information was not developed prior to the data that the control algorithm needed to be operational. The steady-state characterization data and a first order dynamical model were utilized as input to a computer program that obtained a solution to the discrete-time Riccati equation. The optimal control law associated with this calculation is given by Table 4. First order response data are illustrated in Figure 1. The SSC-2 was inserted at 1148 on June 1, 1981, and the temperatures in the capsule were adjusted and balanced in the manual mode. Computer control for the capsule was initiated June 2, 1981.

Temperatures and reactor power data from the ORR-PSF pressure vessel capsule irradiation experiment for March 1981 were processed. Cumulative results through March 1981 are shown in Table 5.

Expected Accomplishments in the Next Reporting Period

Data from SSC-2 and the pressure vessel will be processed and reported in monthly highlights as it becomes available from the dedicated computer system.

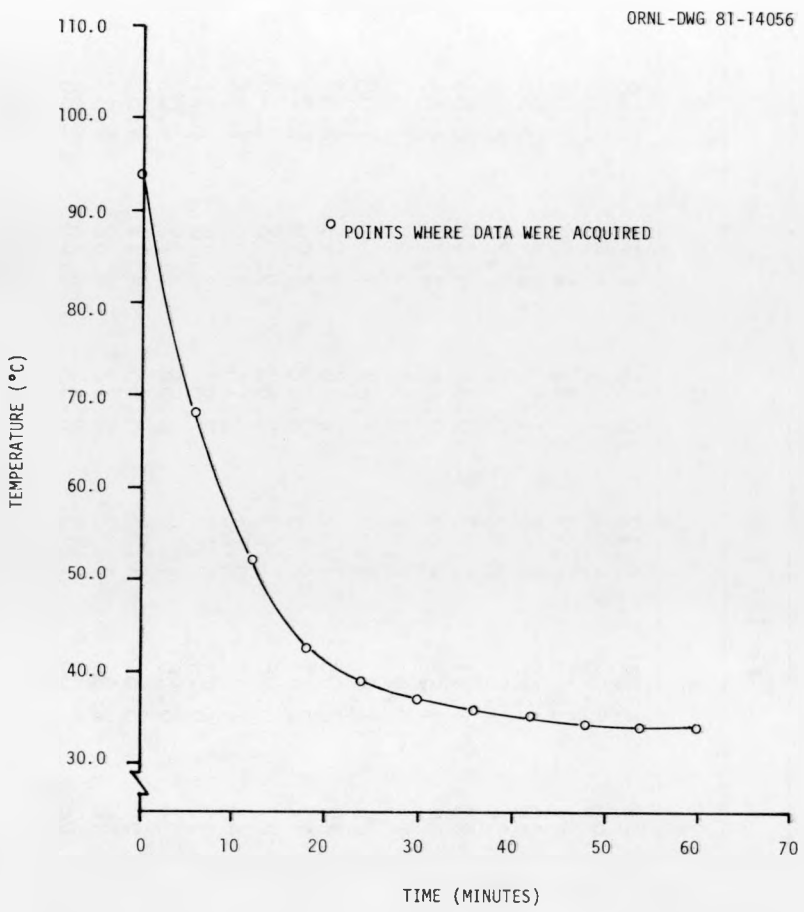

Figure ORNL-1. Response of TE-1 After Electrical Heater Power is Turned Off. Note that the first order time constant is approximately ten minutes. Other thermocouples respond with essentially the same characteristics.

Table ORNL-3

Change in Thermocouple Temperature (°C) Due to a One Hundred Watt Power Change of a Single Heater. Actual power changes in watts are listed in the last entry of the table.

Thermocouple	Heater Number									
	1	2	3	4	5	6	7	8	9	10
TE 1	0.76	1.24	2.87	5.84	8.12	0.96	1.72	2.58	6.36	7.91
TE 2	1.01	1.71	3.90	6.08	5.86	1.19	1.59	2.83	6.61	5.99
TE 3	1.01	1.60	3.67	3.40	7.99	1.43	1.84	3.08	3.55	8.42
TE 4	1.14	2.65	5.40	2.47	5.73	1.19	2.47	3.96	2.57	5.61
TE 5	1.14	2.88	4.36	1.54	8.62	0.60	2.73	2.46	1.23	7.91
TE 6	1.01	5.00	3.90	1.31	5.73	0.48	4.49	2.83	0.98	5.22
TE 7	1.26	4.76	2.75	1.54	6.99	0.48	4.74	1.45	0.37	7.01
TE 8	2.52	2.06	4.13	10.9	2.35	3.10	2.22	3.33	1.25	2.55
TE 9	2.64	2.18	4.25	11.8	2.48	2.62	1.97	3.08	11.0	2.42
TE10	2.27	3.47	6.43	2.93	1.35	2.38	3.99	5.84	2.32	2.17
TE11	2.27	3.12	7.12	2.47	2.10	2.62	3.99	5.71	2.69	2.80
TE12	1.89	7.82	2.87	0.96	1.23	2.62	9.93	2.46	0.74	1.91
TE13	2.77	9.47	3.44	1.42	2.23	2.15	8.29	1.95	0.49	1.40
TE14	8.57	2.88	3.33	6.54	1.23	7.87	2.73	2.71	5.63	1.02
TE15	6.30	3.59	4.94	6.66	1.10	6.56	3.73	4.08	6.36	1.53
TE16	8.32	3.12	3.56	3.86	1.35	8.35	4.11	3.58	3.79	0.90
TE17	6.17	4.06	5.40	2.93	1.23	6.32	4.62	4.33	2.69	1.28
TE18	8.70	4.65	4.02	2.00	1.10	8.35	4.62	3.08	1.35	1.15
TE19	6.42	6.29	4.25	1.77	1.48	5.84	6.13	2.83	0.98	1.02
TE20	7.81	5.47	2.52	1.19	1.10	7.75	5.63	2.08	0.86	1.15
Power Change	192.6	206.7	211.3	208.4	193.8	203.5	192.2	193.6	198.2	190.4

Table ORNL-4

Optimal Control Law Matrix Obtained by Solving the Discrete-Time Matrix Riccati Equation

Row Number	Column Numbers									
	1 11	2 12	3 13	4 14	5 15	6 16	7 17	8 18	9 19	10 20
1	.574(−2) −.527(−1)	−.325(−2) −.322(−1)	−.837(−2) −.728(−1)	−.124(−1) −.326(0)	−.182(−1) −.218(0)	−.849(−2) −.315(0)	−.228(−1) −.220(0)	−.508(−1) −.334(0)	−.588(−1) −.234(0)	−.541(−1) −.298(0)
2	−.104(−1) −.917(−1)	−.339(−1) −.307(0)	−.271(−1) −.386(0)	−.769(−1) −.715(−1)	−.872(−1) −.102(0)	−.182(0) −.805(−1)	−.175(0) −.127(0)	−.404(−1) −.152(0)	−.475(−1) −.231(0)	−.111(0) −.194(0)
3	−.715(−1) −.279(0)	−.123(0) −.788(−1)	−.114(0) −.104(0)	−.201(0) −.859(−1)	−.151(0) −.158(0)	−.132(0) −.994(−1)	−.770(−1) −.120(0)	−.118(0) −.125(0)	−.126(0) −.138(0)	−.249(0) −.585(−1)
4	−.240(0) −.594(−1)	−.216(0) −.298(−2)	−.996(−1) −.232(−1)	−.624(−1) −.231(0)	−.225(−1) −.232(0)	−.176(−1) −.113(0)	−.296(−1) −.754(−1)	−.415(0) −.354(−1)	−.461(0) −.302(−1)	−.845(−1) −.523(−2)
5	−.317(0) −.514(−1)	−.217(0) −.169(−1)	−.314(0) −.601(−1)	−.216(0) −.146(−1)	−.347(0) −.110(−2)	−.220(0) −.231(−1)	−.276(0) −.152(−1)	−.496(−1) −.140(−1)	−.570(−1) −.303(−1)	−.196(−1) −.177(−1)
6	−.391(−2) −.702(−1)	−.119(−1) −.691(−1)	−.293(−1) −.443(−1)	−.155(−1) −.293(0)	.696(−2) −.231(0)	.161(−1) −.318(0)	.137(−1) −.228(0)	−.779(−1) −.319(0)	−.568(−1) −.207(0)	−.599(−1) −.297(0)
7	−.319(−1) −.131(0)	−.260(−1) −.407(0)	−.369(−1) −.325(0)	−.660(−1) −.607(−1)	−.781(−1) −.105(0)	−.160(0) −.125(0)	−.173(0) −.150(0)	−.451(−1) −.146(0)	−.344(−1) −.220(0)	−.133(0) −.199(0)
8	−.734(−1) −.226(0)	−.864(−1) −.732(−1)	−.101(0) −.469(−1)	−.145(0) −.713(−1)	−.739(−1) −.134(0)	−.944(−1) −.155(0)	−.281(−1) −.154(0)	−.966(−1) −.939(−1)	−.861(−1) −.844(−1)	−.234(0) −.509(−1)
9	−.229(0) −.734(−1)	−.243(0) .219(−2)	−.108(0) .161(−1)	−.695(−1) −.191(0)	−.997(−2) −.221(0)	−.494(−2) −.115(0)	.239(−1) −.686(−1)	−.493(0) −.974(−2)	−.423(0) .232(−2)	−.581(−1) .487(−2)
10	−.307(0) −.849(−1)	−.223(0) −.502(−1)	−.335(0) −.232(−1)	−.211(0) −.417(−2)	−.313(0) −.215(−1)	−.196(0) −.993(−3)	−.277(0) −.175(−1)	−.584(−1) −.166(−1)	−.533(−1) −.822(−2)	−.590(−1) −.205(−1)

Table ORNL-5

Cumulative Characterization Data for the Pressure Vessel Capsule Through March 31, 1981

Data for PSF Specimen Set OT
Hours of Irradiation = 5962.06
Megawatt Hours of Irradiation = 169088.34

Thermocouple	Hours of Irradiation					Average	Standard
	T<270	270<T<280	280<T<296	296<T<306	306<T	Temperature	Deviation
TE 101	62.12	23.38	5855.18	21.38	0.00	289.60	1.75
TE 102	58.55	17.73	5841.03	44.73	0.00	291.45	1.36
TE 103	58.22	16.04	5887.79	0.00	0.00	289.30	1.01
TE 104	52.94	13.57	5826.02	69.52	0.00	292.18	1.11
TE 105	56.88	19.19	5886.01	0.00	0.00	285.83	1.12
TE 106	52.89	14.41	5894.73	0.00	0.00	288.90	1.14
TE 107	58.26	376.90	5526.91	0.00	0.00	282.26	1.39
TE 108	65.72	18.57	5868.65	9.06	0.00	289.27	1.62
TE 109	65.88	19.43	5868.94	7.78	0.00	288.88	1.67
TE 110	58.11	18.01	5873.00	12.95	0.00	290.09	1.30
TE 111	131.68	20.23	5810.12	0.00	0.00	287.88	1.44
TE 112	1.75	0.00	5960.28	0.00	0.00	288.00	0.00
TE 113	52.03	15.31	5892.64	0.04	2.00	289.96	1.68
TE 114	69.95	18.61	5873.47	0.00	0.00	288.72	1.50
TE 115	4.08	0.00	5957.95	0.00	0.00	288.00	0.00
TE 116	64.53	13.41	5884.10	0.00	0.00	290.07	0.86
TE 117	58.39	16.47	5881.37	5.29	0.50	291.23	0.94
TE 118	61.21	22.39	5878.51	0.00	0.00	286.49	1.01
TE 119	58.28	19.94	5883.83	0.00	0.00	286.52	1.03
TE 120	63.83	199.31	5698.97	0.00	0.00	283.14	1.42

Data for PSF Specimen Set 1/4T
Hours of Irradiation Time = 5962.06
Megawatt Hours of Irradiation = 169088.34

TE 201	62.71	18.61	5878.08	2.66	0.00	290.36	1.46
TE 202	62.98	17.12	5881.77	0.17	0.00	288.89	0.96
TE 203	61.61	14.37	5886.10	0.00	0.00	288.64	1.07
TE 204	58.70	15.29	5887.74	0.33	0.00	289.30	0.86
TE 205	58.53	22.34	5881.20	0.00	0.00	286.33	1.05
TE 206	56.64	20.55	5884.87	0.00	0.00	286.74	0.91
TE 207	61.50	86.13	5814.45	0.00	0.00	282.97	1.08
TE 208	64.11	14.56	5882.53	0.83	0.00	288.15	1.33
TE 209	64.76	19.59	5875.70	2.00	0.00	288.79	1.27
TE 210	63.69	28.74	5869.63	0.00	0.00	286.34	0.96
TE 211	67.31	32.40	5862.34	0.00	0.00	284.47	0.84
TE 212	56.11	10.20	5895.73	0.00	0.00	290.69	1.04
TE 213	56.47	10.80	5894.76	0.00	0.00	289.30	1.15
TE 214	64.93	12.26	5884.84	0.00	0.00	290.49	0.96
TE 215	64.89	19.45	5877.67	0.00	0.00	287.42	0.71
TE 216	63.68	14.11	5884.27	0.00	0.00	287.87	0.77
TE 217	60.20	11.54	5890.31	0.00	0.00	289.49	0.95
TE 218	60.12	17.26	5882.69	2.00	0.00	286.89	0.98
TE 219	58.66	14.46	5888.95	0.00	0.00	286.99	0.87
TE 220	59.74	107.68	5794.64	0.00	0.00	285.40	1.20

Table ORNL-5 (Cont'd)

Data for PSF Specimen Set 1/2T
Hours of Irradiation = 5962.06
Megawatt Hours of Irradiation = 169088.34

Thermocouple	Hours of Irradiation					Average Temperature	Standard Deviation
	T<270	270<T<280	280<T<296	296<T<306	306<T		
TE 301	62.03	9.58	5851.30	39.18	0.00	290.27	1.05
TE 302	64.28	15.14	5882.65	0.00	0.00	286.49	0.81
TE 303	61.35	11.17	5889.53	0.00	0.00	287.27	0.90
TE 304	56.61	11.61	5893.24	0.58	0.00	290.94	0.79
TE 305	56.30	12.69	5893.03	0.03	0.00	287.59	0.91
TE 306	59.43	17.48	5885.14	0.00	0.00	286.52	0.82
TE 307	1.75	0.00	5960.28	0.00	0.00	288.00	0.00
TE 308	64.22	9.61	5888.21	0.00	0.00	289.07	1.14
TE 309	65.60	12.82	5883.65	0.00	0.00	287.69	0.86
TE 310	67.48	31.16	5863.43	0.00	0.00	285.23	1.09
TE 311	67.32	31.46	5863.32	0.00	0.00	285.69	1.15
TE 312	59.26	9.00	5893.62	0.17	0.00	288.74	0.93
TE 313	58.88	9.27	5892.24	1.67	0.00	290.10	1.01
TE 314	66.66	11.64	5883.74	0.00	0.00	289.22	1.02
TE 315	68.38	13.22	5880.46	0.00	0.00	285.11	0.89
TE 316	64.73	6.97	5890.37	0.00	0.00	287.60	0.72
TE 317	58.15	12.44	891.47	0.00	0.00	290.74	0.87
TE 318	57.75	11.86	5892.43	0.00	0.00	289.23	0.96
TE 319	62.99	18.45	5880.60	0.00	0.00	285.27	0.78
TE 320	60.70	14.37	5886.97	0.00	0.00	287.81	1.21

A.3 Surveillance Dosimetry Measurement Benchmark Facility (SDMF) for Validation and Certification of Neutron Exposures from Power Reactor Surveillance

Accomplishments and Status

A preliminary program plan for the characterization of the SDMF was drawn up for discussion. A tentative time table and cost estimates were proposed. E. D. McGarry from NBS will coordinate with the vendors to obtain sketches of the surveillance capsule used in their respective reactors.

Expected Accomplishments in the Next Reporting Period

Two or three generic surveillance capsules will be selected for use in the SDMF.

B. ASTM STANDARDS FOR SURVEILLANCE OF NUCLEAR REACTOR PRESSURE VESSELS

F. B. K. Kam
F. W. Stallmann
L. F. Miller

Objectives

The primary objective of the LWR Pressure Vessel Surveillance Dosimetry program is to prepare an updated and improved set of dosimetry, damage correlation, and associated reactor analysis ASTM Standards to predict the integrated effect of neutron exposure to LWR pressure vessels and support structures.

Accomplishments and Status

The "ASTM Standard Guide for Application of Neutron Transport Methods for Reactor Vessel Surveillance" received three negative votes in the E10.05 ballot procedure. Tentative agreement has been reached to resolve the negatives.

A general paper on the "Theory and Practice of General Adjustment and Model Fitting Procedures" has been completed by F. W. Stallmann. The theory of ORNL's current log-normal least square adjustment code LSL is described in the above paper.

A draft of a "New Standard Recommended Practice for the Application of Neutron Spectrum Adjustment Methods in Reactor Surveillance" was submitted to ASTM Subcommittee E10.05 for comments. Pertinent comments will be submitted to the E10.05 Subcommittee for ballot before the January 1982 ASTM meeting in Houston, Texas.

Expected Accomplishments During the Next Reporting Period

The "ASTM Standard Guide for Application of Neutron Transport Methods for Reactor Vessel Surveillance" will be ready for E10 balloting.

The "Standard Recommended Practice on Adjustment Procedures" will be ready for E10.05 balloting.

F. W. Stallmann's paper on the "Theory and Practice of General Adjustment and Model Fitting Procedures" will be published as NUREG/CR-2222, ORNL/TM-7896.

NAVAL RESEARCH LABORATORY
(NRL)

A. POSTIRRADIATION NOTCH DUCTILITY OF STEEL PLATES, WELDS AND FORGING FROM SURVEILLANCE SPECIMEN CAPSULE NO. 1

J. R. Hawthorne (NRL)

Objective

To determine the degradation of notch ductility produced in steel by the neutron exposure conditions of Simulated Surveillance Capsule No. 1 that was irradiated in the Oak Ridge Research Reactor Pool Side Facility.

Summary

Six pressure vessel steel materials provided by the United States and European laboratories to the NRC LWR-PVI Surveillance Dosimetry Program are being irradiated in the Oak Ridge Research Reactor (ORR) Pool Side Facility (PSF) for determinations of radiation-induced change in notch ductility, fracture toughness and strength properties as functions of neutron spectra and fluence conditions. Notch ductility determinations are reported for Simulated Surveillance Capsule No. 1 (SSC-1) the first materials experiment discharged from the PSF. Results indicate a broad range of radiation embrittlement sensitivities for the materials consistent with individual material copper and nickel contents.

Accomplishments and Status

Introduction

The Naval Research Laboratory (NRL) was assigned the primary responsibility for testing the Charpy-V (C_V), compact tension (CT), and tension (T) specimens being irradiated in experiment assemblies in the NRC Pool Side Facility (PSF). Specimen test materials include plate, forging, and submerged arc weld deposit materials provided to the LWR-PVI Surveillance Dosimetry program by six organizations in the USA and overseas.

Simulated Surveillance Capsule No. 1 (SSC-1) represents the first materials experiment discharged from the PSF. The SSC-1 was irradiated at 288°C (nominal) for 1075.29 hours (~45 days) at a location adjacent to the simulated thermal shield. Estimated neutron fluences for individual specimens exceed 2×10^{19} n/cm^2, E >1 MeV.

Postirradiation Testing

Postirradiation C_v tests have been completed for all SSC-1 materials. The materials evaluated include A302-B and A533-B reference plates, A508 Class 2 and Class 3 forgings and two submerged arc welds. Experimental results are given in Figs. 1 to 6. By convention, open symbol points indicate unirradiated condition data; filled symbol points refer to the irradiated condition. Also, filled circle and filled square symbols, respectively, represent specimens contained in left and right hand specimen compartments of the SSC-1 assembly.

Material Code F23 (ASTM A302-B Reference Plate, NRL Supplier)

Postirradiation C_v test results for this plate are given in Fig. 1. Data for the unirradiated condition are also shown in this figure and were developed using the same (in cell) test machine. Unirradiated condition specimens were from the same section of plate and plate thickness location as the SSC-1 specimens.

The experimental results may be summarized as follows:

1. Specimens contained in the left hand (group 1) and right hand (group 2) compartments of the SSC-1 indicate a difference in postirradiation notch ductility. The low data scatter suggests that the difference is real. The occurrence of two separate data patterns cannot be attributed to neutron fluence dissimilarities but may be a reflection of specimen locations in the parent plate. Specimens forming group 1 were from plate thickness layer 1 only; specimens forming group 2 were from plate thickness layer 2 only. Unirradiated condition tests of these two adjacent thickness layers indicated identical properties. Thus, the postirradiation difference, especially that at upper shelf temperatures, is considered anomalous at this time.

2. C_v 41J (30 ft-lb) transition temperature elevations for the measured fluence level are in good agreement with the 288°C irradiation data trend established previously for this steel (see Fig. 7)[1].

Material Code 3PU (A533-B Class 1 Reference Plate, HSST 03, ORNL Supplier)

The C_v notch ductility behavior of this plate before and after irradiation is illustrated in Fig. 2. Unlike the A302-B plate above, the data describe a single data trend independent of SSC-1 compartment location. With two exceptions, the data scatter is relatively small. The C_v 41J temperature elevation is less than that for the A302-B reference plate. The smaller irradiation effect is consistent with the lower neutron fluence and copper content of this material. In a separate study, irradiation of the A533-B plate at 288°C to 2.1×10^{19} n/cm^2 >1 MeV in the State University of New York at Buffalo Reactor (UBR) produced a transition temperature elevation of 44°C (80°F). Noting the fluence level, the determination for an in-core irradiation is in good agreement with the present determination for the out-of-core SSC-1 experiment.

Material Code MO (A508 Class 3 Forging, MOL Supplier)

At MOL and NRC request, NRL performed preirradiation as well as postirradiation tests for this material. The reference tests were intended to supplement MOL unirradiated condition data and to enable direct comparisons with postirradiation data. Again, the same (in-cell) machine was used for both material conditions. Experimental results are shown in Fig. 3 and permit the following observations:

1. Data for the reference condition obtained independently by NRL are in very good agreement with the MOL data over the full test temperature range.

2. Data scatter is evident; however, there is not a major difference between forging test layers (inside versus outside).

3. Data from experiment SSC-1 specimens overlap within the scatterband of data for the unirradiated condition. (Hardness values for unirradiated and irradiated conditions are also about the same).

4. On the basis of (3), this material is judged to have high resistance to the neutron fluence received.

As an additional observation, the irradiation data do not show a difference between left and right hand specimen groups in the SSC-1 unit. On the other hand, we would not expect a pronounced difference in view of the high radiation resistance of the forging. Because the property changes with irradiation to $\sim 2 \times 10^{19}$ n/cm^2 were essentially nil, we can expect that lower fluence irradiations of this material also will have no significant effect on C_v properties. In turn, postirradiation testing of the Code MO C_v specimens from the lower fluence PSF experiments may not be necessary.

Material Code K (22NiMoCr37 Forging, KFA Supplier)

Postirradiation test results are given in Fig. 4. In this case, only two data points for the unirradiated condition were supplied to NRL for assessments of the irradiation effect. Data for the irradiated and reference conditions, however, appear to overlap. Accordingly, this forging, like the forging Code MO, is judged to have high radiation resistance at 288^{o}C. If confirmed, tests from lower fluence experiments again may not be necessary. Confirmation will require the receipt of additional data for the reference condition.

Material Code EC (Submerged Arc Weld, EPRI Supplier)

Figure 5 presents the postirradiation data developed for the SSC-1 experiment and a trend curve obtained for a lower fluence exposure of the weld by the NRL-EPRI RP886-2 Program.[2] Primary observations are as follows:

1. The radiation embrittlement described by both data sets is significant and is consistent with the relatively high copper content ($\sim$0.22%Cu) of the weld.

2. The respective upper shelf reductions and transition temperature elevations describe a trend of increasing irradiation damage with fluence.

3. The exposure conditions produced a relatively low C_v upper shelf energy level. The trend of the upper shelf reduction will be of particular interest in forthcoming PSF experiments.

4. Transition temperature elevations indexed by the 0.89 mm (35 mils) lateral expansion temperature are slightly higher than those indexed by the 41J (30 ft-lb) temperature.

5. A postirradiation lateral expansion of 0.94 mm (37 mils) equates to 58J (43 ft-lb) energy absorption and not 68J (50 ft-lb) for this particular weld.

Weld Code R (Submerged Arc Weld, Rolls Royce Supplier)

Test results for the Code R weld are given in Fig. 6. Evaluations of the data indicate:

1. The Code R weld is the most radiation sensitive of all the materials evaluated from the SSC-1 experiment.

2. The high radiation sensitivity is consistent with the high copper content (0.24%Cu) and the high nickel content (1.58%Ni) of the weld.

3. The postirradiation C_v upper shelf level exceeds 68J (50 ft-lb) in contrast to the low upper shelf level of the Code EC weld.

4. The postirradiation upper shelf qualities of the weld, in part, is a reflection of its high preirradiation upper shelf level.

Discussion

The radiation degradations for the forgings and one of the two welds evaluated are either significantly less or significantly greater than that ob served for the ASTM A302-B reference plate or the HSST A533-B reference plate. The exception is the submerged arc weld, Code EC. The 41J transition temperature elevation of this weld ($108^{o}C$) was similar to determinations made for the ASTM A302-B reference plate (78 and $86^{o}C$); the postirradiation upper shelf energy reduction (34J, 25 ft-lb) was also about the same as that for this plate. Material performances appear to be directly related to copper content and possibly nickel content.

Expected Achievements in Next Reporting Period

Postirradiation tests of tensile specimens from the SSC-1 are scheduled for completion by 30 September 1981. Tests of unirradiated condition C_v specimens of Code K material (just received) are also to be completed within the next reporting period.

References

1. J. R. Hawthorne, J. J. Koziol and S. T. Byrne, "Evaluation of Commercial Production A533-B Steel Plates and Weld Deposits with Extra-Low Copper Content for Radiation Resistance," NRL Report 8136, Naval Research Laboratory, October 21, 1977.

2. J. R. Hawthorne (Ed.), "The NRL-EPRI Research Program (RP886-2), Evaluation and Prediction of Neutron Embrittlement in Reactor Pressure Vessel Materials, Annual Progress Report for CY 1979, Part I. Dynamic C_v, PCC_v Investigations," NRL Memorandum Report 4431, Naval Research Laboratory, December 31, 1980.

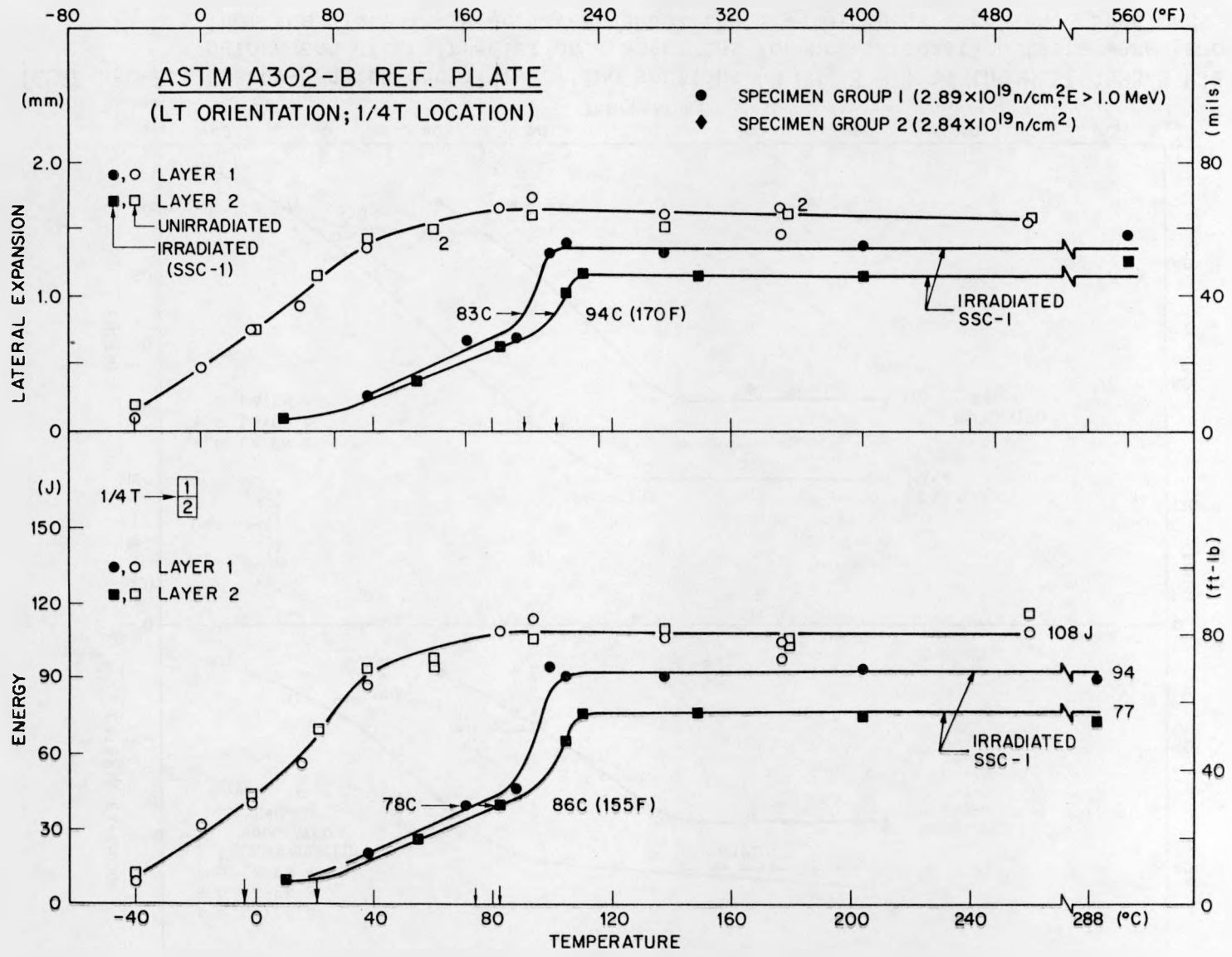

FIGURE NRL-1. Charpy-V notch ductility of section F23 of the ASTM A302-B reference plate before and after irradiation. Specimens for pre-irradiation and postirradiation determinations were removed from the plate in two layers spanning the 1/4-thickness location (SSC-1 experiment).

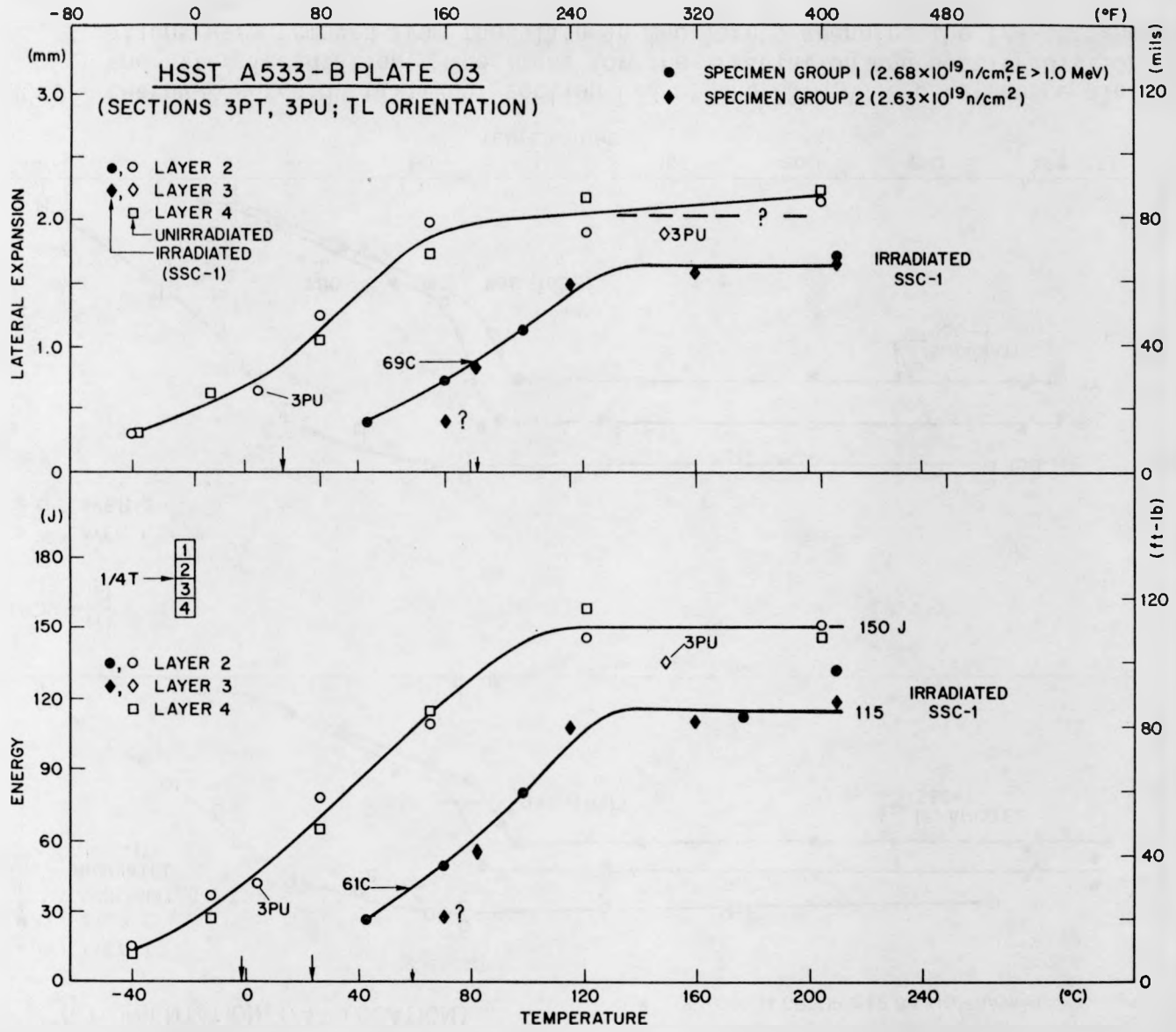

FIGURE NRL-2. Charpy-V notch ductility of two sections (3 PU, 3 PT) of the HSST A533-B Plate 03 before and after irradiation. Specimens for pre-irradiation tests were removed from the plate in three layers about the 1/4-thickness location. Specimens for postirradiation tests were taken from layers 2 and 3 only (SSC-1 experiment).

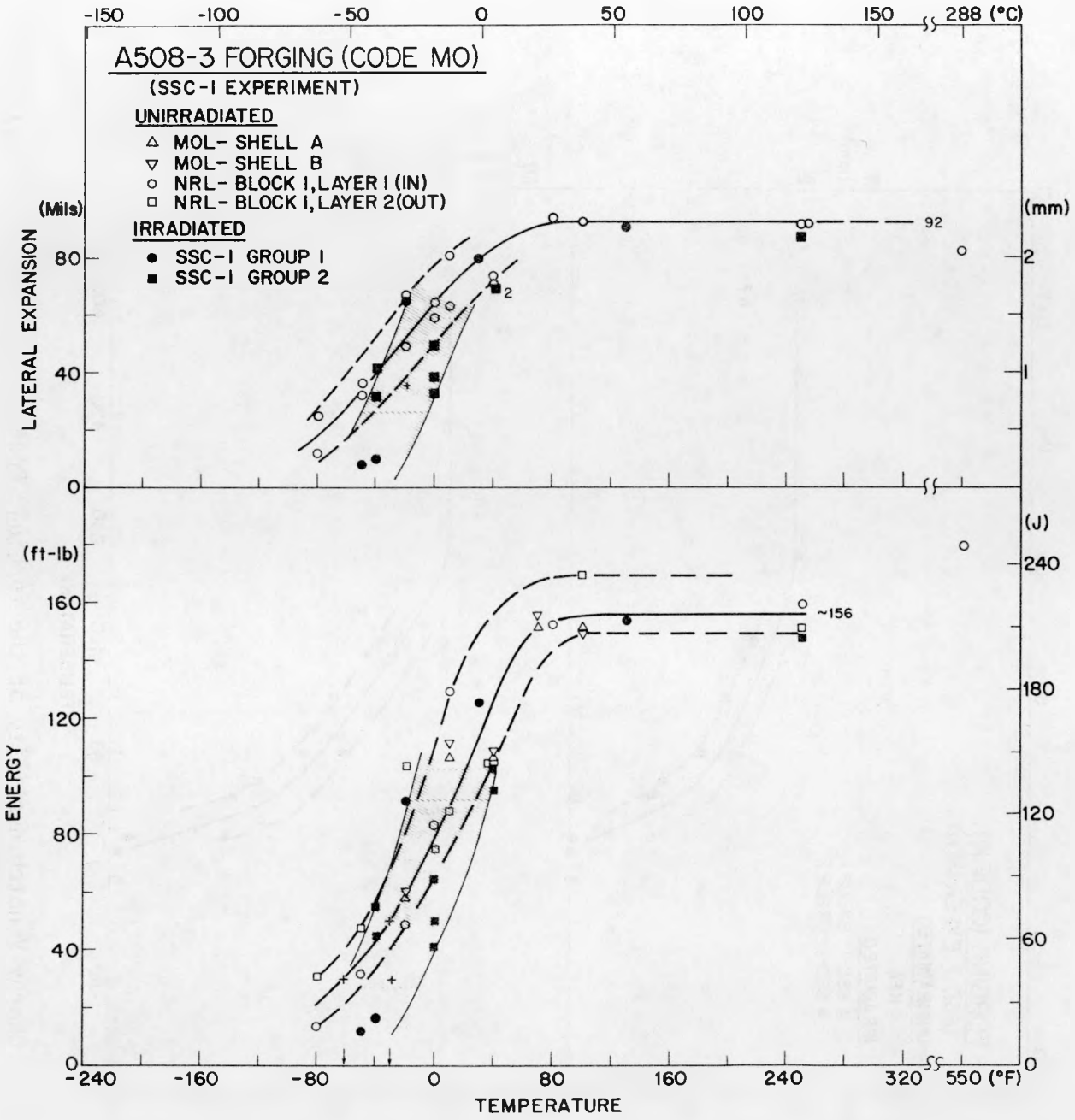

FIGURE NRL-3. Charpy-V notch ductility of the forging, Code MO, before and after irradiation (SSC-1 experiment).

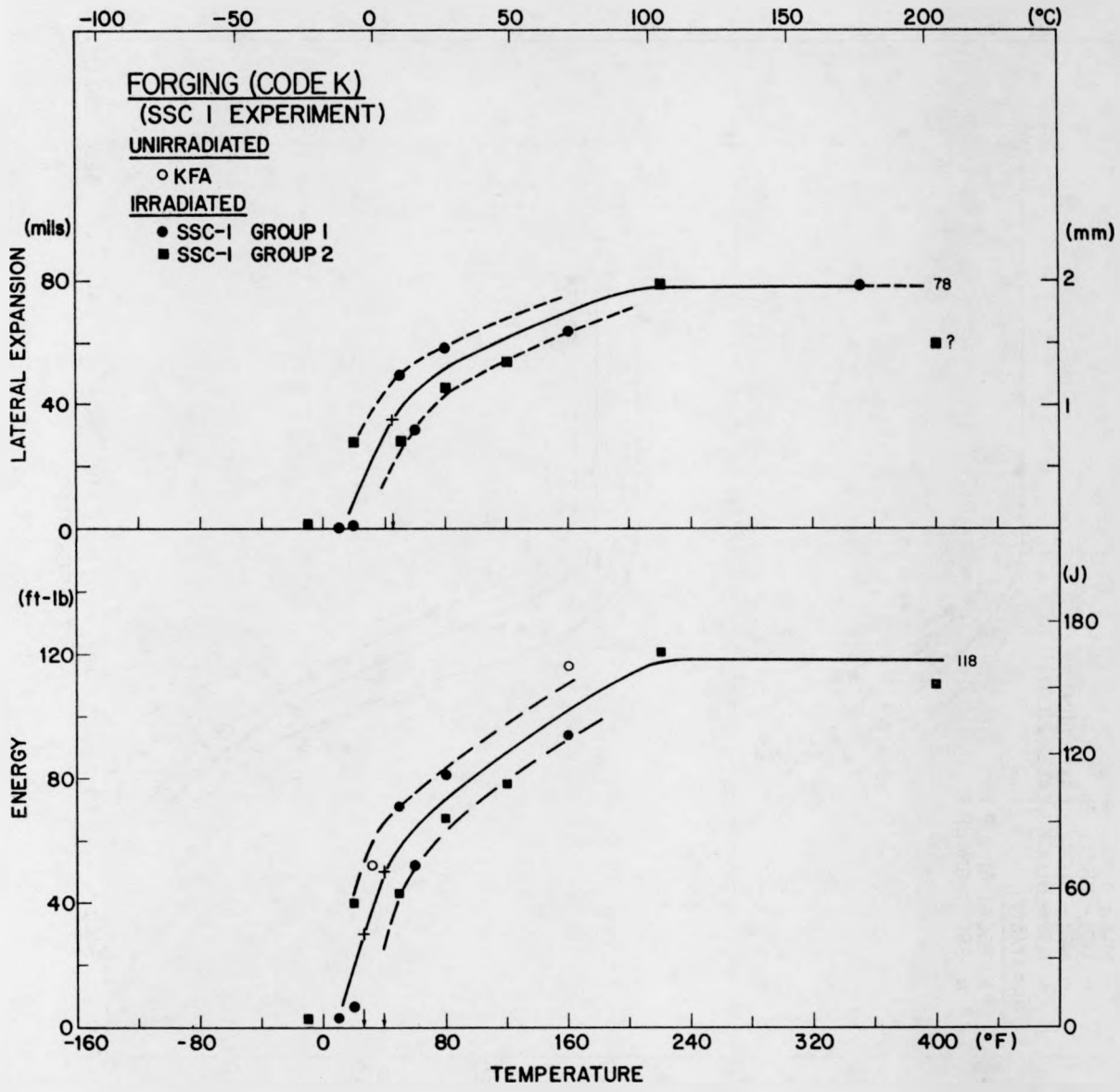

FIGURE NRL-4. Charpy-V notch ductility of the forging, Code K, before and after irradiation (SSC-1 experiment).

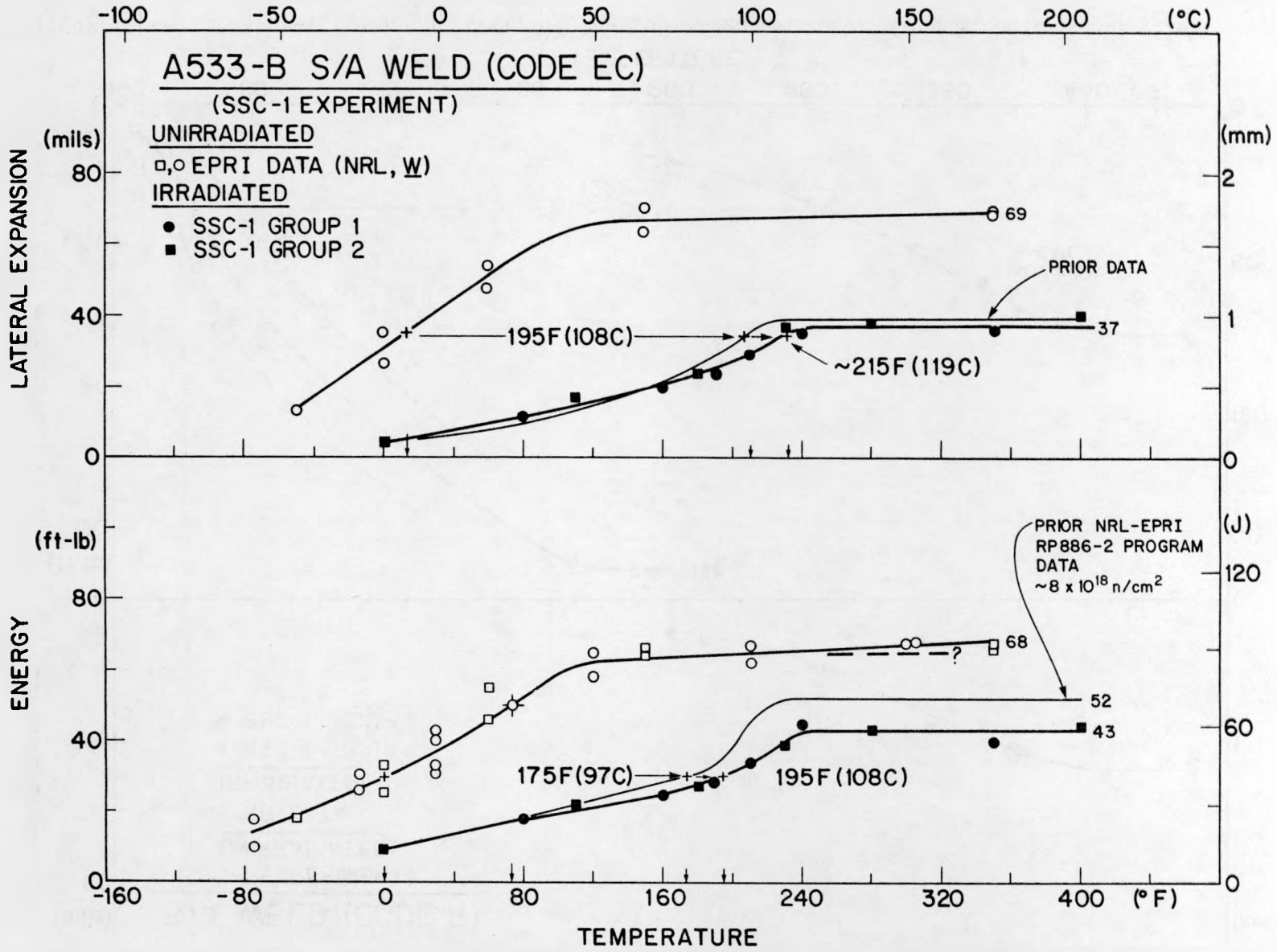

FIGURE NRL-5. Charpy-V notch ductility of the submerged arc weld, Code EC, before and after irradiation to two fluence levels (SSC-1 experiment and NRL-EPRI experiment BSR 12).

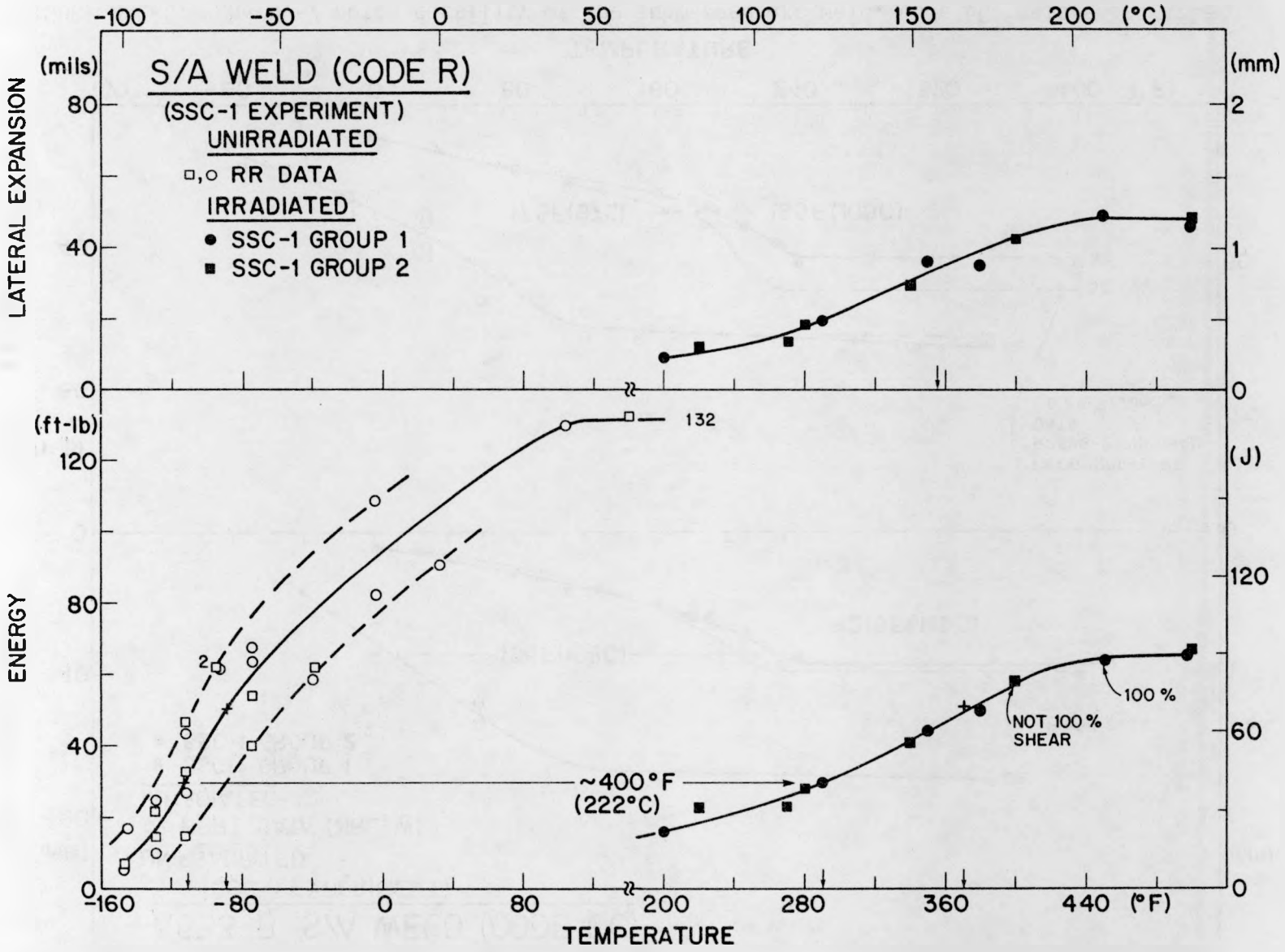

FIGURE NRL-6. Charpy-V notch ductility of the submerged arc weld, Code R, before and after irradiation (SSC-1 experiment).

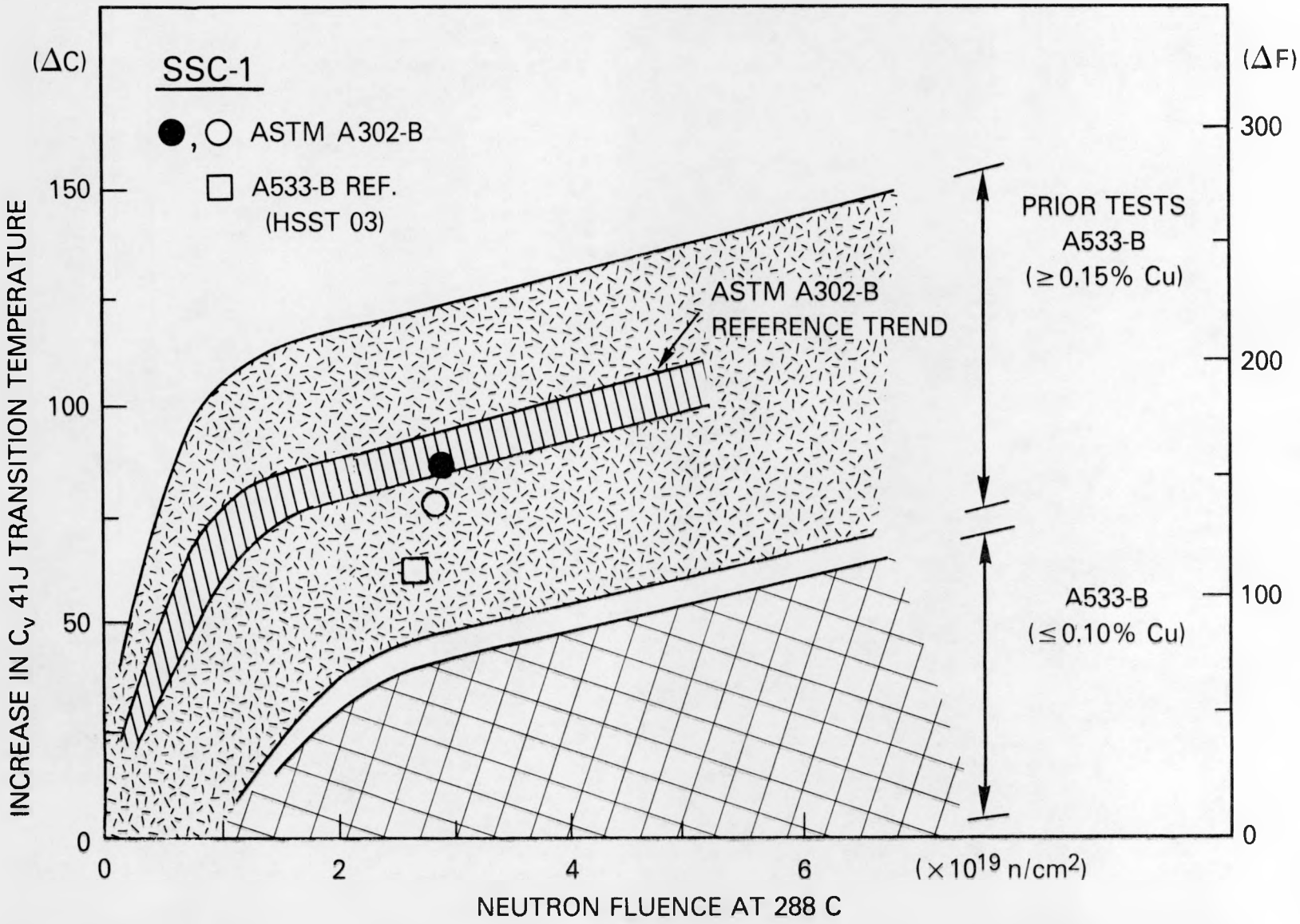

FIGURE NRL-7. Postirradiation transition temperature elevations for the ASTM A302-B and A533-B reference plates compared to prior observations on material trends with 288°C test reactor irradiation experiments.